Glucocorticoid-induced leucine zipper protein regulates sodium and potassium balance in the distal nephron

Priyanka Rashmi[1], **GianLuca Colussi**[2], **Michael Ng**[1], **Xinhao Wu**[1], **Atif Kidwai**[1], and **David Pearce**[1,*]

[1]Division of Nephrology, Department of Medicine, University of California, San Francisco, California 94143, USA

Abstract

Glucocorticoid induced leucine zipper protein (GILZ) is an aldosterone-regulated protein that controls sodium transport in cultured kidney epithelial cells. Mice lacking GILZ have been reported previously to have electrolyte abnormalities. However, the mechanistic basis has not been explored. Here we provide evidence supporting a role for GILZ in modulating the balance of renal sodium and potassium excretion by regulating the sodium-chloride cotransporter (NCC) activity in the distal nephron. GILZ–/– knockout mice have a higher plasma potassium concentration and lower fractional excretion of potassium than wild type mice. Furthermore, knockout mice are more sensitive to NCC inhibition by thiazides than are the wild type mice, and their phosphorylated NCC expression is higher. Despite increased NCC activity, knockout mice do not have higher blood pressure than wild type mice. However, during sodium deprivation, knockout mice come into sodium balance *more quickly*, than do the wild type, without a significant increase in plasma renin activity. Upon prolonged sodium restriction, knockout mice develop frank hyperkalemia. Finally, in HEK293T cells, exogenous GILZ inhibits NCC activity at least in part by inhibiting SPAK phosphorylation. Thus, GILZ promotes potassium secretion by inhibiting NCC and enhancing distal sodium delivery to the epithelial sodium channel. Additionally, *Gilz* knockout mice have features resembling familial hyperkalemic hypertension, a human disorder that manifests with hyperkalemia associated variably with hypertension.

Keywords

aldosterone; distal tubule; hypernatremia; potassium channels

---

*Corresponding author: David Pearce, M.D., University of California San Francisco, 600 16th St., San Francisco, CA 94143. David.Pearce@ucsf.edu.
[2]Current location: Department of Experimental and Clinical Medical Sciences, University of Udine, Udine, Italy.

Introduction

The kidney, in particular the aldosterone-sensitive distal nephron (ASDN), plays a critical role in regulating potassium (K^+) and sodium (Na^+) flux to achieve homeostasis of body fluid volume and plasma K^+ concentration $[K^+]$.[1] Plasma $[K^+]$ is maintained within an extremely tight range in humans and mice.[2] Abnormalities in plasma $[K^+]$ can alter cellular electrical excitability with the potential of causing life-threatening cardiac arrhythmias.[3] On the other hand, the Na^+ balance of the body is critical for the maintenance of extracellular fluid (ECF) volume and a normal blood pressure (BP).[4]

Aldosterone is a key hormone that orchestrates Na^+ and K^+ balance in response to environmental conditions, particularly changes in dietary Na^+ and K^+ availability, by inducing the expression of target genes such as Glucocorticoid induced leucine zipper protein (GILZ) and Serum and Glucocorticoid-regulated kinase 1 (SGK1). These gene products and their downstream signaling pathways further modulate the synthesis, trafficking, stability, and intrinsic activity of various ion transporters and channels.[5, 6] In the distal convoluted tubule (DCT), Na^+ is reabsorbed predominantly by the electroneutral Na-Cl cotransporter (NCC) and in the connecting tubule and collecting duct by the electrogenic epithelial sodium channel (ENaC). ENaC mediated sodium reabsorption depolarizes the apical membrane, generating a lumen negative voltage that provides the electrical driving force for K^+ secretion.[7] Recent studies have increasingly supported a role for the coordinated regulation of electroneutral and electrogenic Na^+ transport in the distal nephron in controlling Na^+ and K^+ balance.[8] Electroneutral reabsorption of Na^+ via NCC does not stimulate K^+ secretion, but in fact inhibits K^+ secretion by competing with ENaC-mediated Na^+ reabsorption.[9] During Na^+ depletion, aldosterone increases Na^+ reabsorption without stimulating K^+ secretion, and there is increasing evidence for a model in which the WNK kinase network integrates systemic volume and K^+ status to fine tune NCC, ENaC, and possibly ROMK activities.[8, 10] It is postulated that, a high concentration of circulating angiotensin II during Na^+ depletion activates the WNK1/4 [With No Lysine (K)]-SPAK (STE20/SPS1-related proline/alanine-rich kinase)-NCC pathway, thus favoring electroneutral Na^+ reabsorption.[11] It has been suggested that aldosterone also acts through the mineralocorticoid receptor (MR) and SGK1 to stimulate NCC.[12] However, this explanation cannot fully explain how plasma K^+ concentrations are maintained in the context of prolonged sodium deficiency as hyperkalemia would eventually develop due to reduced Na^+ delivery to the ENaC-expressing nephron segments, resulting in reduced K^+ secretion. Therefore, understanding the intracellular signaling networks and identifying novel mediators that play a key role in striking an appropriate balance between electroneutral and electrogenic Na^+ transport in the distal renal tubule in response to systemic inputs including volume status, K^+ status, and aldosterone is critical.

GILZ is a member of the transforming growth factor (TGF) β-stimulated clone 22 domain (TSC22D) family.[13] So far, four GILZ isoforms have been identified; but only isoform 1 (GILZ1) stimulates ENaC mediated Na^+ current in mpkCCD$_{c14}$ cells and *Xenopus laevis* oocytes.[14] GILZ1 expression is strongly induced by aldosterone in kidney as well as in mpkCCD$_{c14}$ cells.[15] In *in vitro* models, GILZ1 physically interacts with and inhibits Raf-1, leading to ENaC activation.[16] GILZ1 also physically interacts with other components of

ENaC regulatory complex; in particular SGK1.[17] GILZ1 increases SGK1 association with key substrates Nedd4-2 and Raf-1, as well as ENaC, while protecting SGK1 from rapid ER-associated proteasome-mediated degradation.[16, 17] In spite of the extensive *in vitro* data, the role of GILZ in mediating ion transport *in vivo* remains unclear, and its role in NCC regulation, in particular, has not been examined.

As of now, we are aware of three distinct *Gilz* knockout (*Gilz*$^{-/-}$) mouse strains that have been characterized (Suarez,[18] Bruscoli,[19, 20] present work) and used to evaluate different GILZ functions. Based on *in vitro* studies, which showed that GILZ stimulates ENaC mediated sodium current and modulates T-cell activation,[13, 15, 21] it was expected that *Gilz*$^{-/-}$ mice would exhibit signs of type 1 pseudohypoaldosteronism (PHA1) and defects in T-cell mediated immunity. Surprisingly, *Gilz*$^{-/-}$ males are sterile due to impaired spermatogenesis but display no tendency to Na^+ wasting and no obvious defects in immune function.[18, 19] However, minor but consistent defects in Na^+ and K^+ handling have been reported.[18] The aim of our present study was to determine whether GILZ regulates whole-animal Na^+ and K^+ balance, and if so, to begin to assess the physiological conditions, the transporters involved and the underlying signaling mechanisms. We have generated a whole body *Gilz*$^{-/-}$ mouse and used a series of evocative tests to study the involvement of GILZ in ion transport regulation. Interestingly, unlike the PHA1 phenotype of SGK1-deficient animals, the phenotype of *Gilz*$^{-/-}$ mice resembles familial hyperkalemic hypertension (FHHt)/type 2 pseudohypoaldosteronism (PHA2), resulting from hyperactivation of WNK-SPAK-NCC pathway. Our data support the idea that a major role of GILZ is to inhibit WNK-SPAK mediated activation of NCC, and thereby prevent the development of hyperkalemia in Na^+-avid states.

Results

Generation of *Gilz*$^{-/-}$ mice

To address GILZ function *in vivo*, we generated mice constitutively deficient for all known TSC22D3-2 isoforms. The strategy for the generation of mice with a *Gilz* knockout allele is described in detail in materials and methods. A previous study used a distinct but similar strategy to constitutively delete *TSC22D3-2*.[18] Consistent with their report, we found that *Gilz*$^{-/-}$ mice are viable, and born with normal body weight, but the males are sterile.[18, 19] The defect in male fertility and failure of sperm maturation was found to be due to the loss of GILZ2 isoform[19] whereas studies in *Xenopus laevis* oocytes and numerous cell lines support a role for GILZ1 in regulation of ENaC.[15] On a normal Na^+ diet (0.49% NaCl), there were no significant differences in the body weight (wild type 24.5 ± 0.6 g *vs.* knockout 24.4 ± 0.5 g, ns); food intake (wild type 3.3 ± 0.1 g/day *vs.* knockout 3.2 ± 0.1 g/day, ns); and water intake (wild type 3.8 ± 0.1 ml/day *vs.* knockout 3.8 ± 0.2 ml/day, ns) between 10–12 weeks old *Gilz*$^{+/+}$ and *Gilz*$^{-/-}$ mice.

Plasma electrolyte abnormalities in *Gilz*$^{-/-}$ mice

First, we examined electrolyte homeostasis and BP in the *Gilz*$^{-/-}$ mice. Comparison of plasma electrolyte levels in *Gilz*$^{-/-}$ mice with those of *Gilz*$^{+/+}$ littermates on a normal Na^+ diet uncovered notable differences in Na^+, K^+, and Cl^- concentrations. Plasma [K^+] in *Gilz*

$^{-/-}$ mice (4.9 ± 0.1 mM) was significantly higher than in $Gilz^{+/+}$ mice (4.3 ± 0.1 mM) (Fig. 1A) consistent with a prior report.[18] In addition, $Gilz^{-/-}$ mice had significantly higher plasma [Na$^+$] levels (Fig. 1B). BP, however, was not significantly different between $Gilz^{+/+}$ and Gilz$^{-/-}$ mice (Table 1). Additionally, there was a modest but significant elevation in plasma [Cl$^-$] (Table 2).

Abnormal renal electrolyte handling in *Gilz$^{-/-}$* mice

Urinary electrolytes showed that despite elevated plasma [K$^+$], $Gilz^{-/-}$ mice showed no increase in urinary K$^+$ excretion, consistent with a renal defect in tubular K$^+$ secretion. This was reflected by a significantly lower fractional excretion of K$^+$ in $Gilz^{-/-}$ mice (Fig. 1C and Table 3). Consistent with the findings of Suarez et al.[18], we did not observe any obvious Na$^+$-excretion defect on a normal salt diet (0.49% NaCl) in $Gilz^{-/-}$ mice (Fig. 1D and Table 3). Additionally, total chloride excretion was significantly reduced in $Gilz^{-/-}$ mice (Table 3). Taken together, the plasma and urinary electrolyte profiles of $Gilz^{-/-}$ mice closely resembled those found in FHHt, and notably the $WNK4^{D561A/+}$ knock-in mouse model reported by Yang et al.[22] Hence, we considered the possibility that WNK-SPAK-NCC pathway could be inappropriately upregulated in $Gilz^{-/-}$ mice.

NCC phosphorylation and functional activity are increased in *Gilz$^{-/-}$* mice

In order to examine the activation state of NCC, we studied its expression and phosphorylation in membrane preparations from kidneys of $Gilz^{+/+}$ and $Gilz^{-/-}$ mice under basal conditions. Phosphorylation of NCC at key activating residues T53 and T58[23] was significantly higher in $Gilz^{-/-}$ mice (Fig. 2). We did not detect any changes in total NCC, full length α-, β-, and γ-ENaC or the proteolytically cleaved fragment of α- and γ-ENaC (Fig. 2 and data not shown). We next examined the natriuretic response to the NCC inhibitor hydrochlorothiazide (HCTZ), which has been used in several studies as a measure of NCC activity.[24] We treated 8–12 week old $Gilz^{+/+}$ and $Gilz^{-/-}$ mice with HCTZ. Consistent with NCC hyperactivity; $Gilz^{-/-}$ mice had a significantly greater natriuretic response to thiazide (Fig. 3A). Short-term treatment with HCTZ also corrected the elevated plasma [K$^+$] and plasma [Na$^+$] (Supplemental Table 1) in $Gilz^{-/-}$ mice. Both $Gilz^{+/+}$ and $Gilz^{-/-}$ mice responded equally to vehicle alone (data not shown). These findings indicate that the phenotypes seen in $Gilz^{-/-}$ mice are dependent upon NCC activity. In contrast, $Gilz^{-/-}$ and $Gilz^{+/+}$ mice had indistinguishable responses to the ENaC inhibitor benzamil suggesting that ENaC activity was similar in the two genotypes (Fig. 3B).

Gilz$^{-/-}$ mice reach sodium balance more rapidly than *Gilz$^{+/+}$* mice on a sodium deficient diet

To further evaluate Na$^+$ handling in $Gilz^{-/-}$ mice, we performed balance cage studies on mice subjected to dietary Na$^+$ restriction. After a three-day lead-in period on normal chow, we placed both $Gilz^{+/+}$ and $Gilz^{-/-}$ mice on a sodium deficient diet (0.01% sodium) for 10 days. Urine was collected at different time points (0–16 h, 16–24 h and thereafter every day). Plasma was collected at 16 h and at the end of 10 days. Surprisingly, $Gilz^{-/-}$ mice excreted significantly less Na$^+$ after 16 h of sodium restriction, compared to $Gilz^{+/+}$ mice (Fig. 4A and Table 4). Between 16 h and 24 h, $Gilz^{+/+}$ and $Gilz^{-/-}$ mice excreted comparable amounts of Na$^+$, and at all subsequent time points, urine Na$^+$ concentration was too low to measure in

both mice. We did not observe any differences in net urinary K^+ excretion between $Gilz^{+/+}$ and $Gilz^{-/-}$ mice either after 16 h or 10 days of sodium deprivation (Table 4). Interestingly, after 10 days on low Na^+ diet, plasma $[Na^+]$ concentration was no longer higher in $Gilz^{-/-}$ mice compared to $Gilz^{+/+}$ as opposed to baseline (Fig. 1B) or 16 h post switching to sodium deficient diet (Fig. 4B). However, the $Gilz^{-/-}$ mice developed frank hyperkalemia at the end of 10 days on sodium deficient diet. While plasma $[K^+]$ trended up in the $Gilz^{+/+}$ mice; it remained significantly lower than the $Gilz^{-/-}$ and within the normal range (Fig. 4C and Table 5). These results suggest that $Gilz^{-/-}$ mice come into sodium balance more quickly than do $Gilz^{+/+}$ mice, but at the expense of developing hyperkalemia. Interestingly, after 16 h of sodium restriction, only the $Gilz^{+/+}$ mice showed a significant rise in PRA. In the $Gilz^{-/-}$ mice, PRA did not rise significantly, consistent with their hypernatriferic state.. After 10 days of low-salt diet, both animals had reached steady state and both had elevated PRA relative to baseline (Fig. 5A). The sodium deficient diet resulted in increased aldosterone levels to the same extent in both $Gilz^{+/+}$ and $Gilz^{-/-}$ mice (Fig. 5B). These results suggest that aldosterone secretion is driven by plasma $[K^+]$ to a greater extent in $Gilz^{-/-}$ than in $Gilz^{+/+}$ mice (see discussion).

Increased NCC and SPAK/OSR1 phosphorylation cascade in $Gilz^{-/-}$ mice

As previously reported, surface expression of activated NCC (phosphorylated at T53 and T58), were increased on low salt diet in $Gilz^{+/+}$ mice (data not shown).[25] Western blot analysis using membrane fractions from kidneys revealed that phosphorylation of NCC at T53 and T58 was significantly higher in $Gilz^{-/-}$ mice relative to that in $Gilz^{+/+}$ mice after 16 h of sodium restriction (Fig. 6). Multiple studies have established a key role for protein kinases SPAK and OSR1 (oxidative stress-responsive kinase 1) in activation of NCC.[25, 26] SPAK and OSR1 can bind and activate NCC by direct phosphorylation of conserved Thr residues: T44, T53 and T58 in its cytoplasmic N-terminal domain.[26–29] SPAK and OSR1 are themselves targets of regulation by WNKs. WNKs constitute a family of kinases vital for the control of ion homeostasis and BP that mediate signaling from activated G protein coupled receptors to downstream effectors.[30–32] Therefore we examined whether this pathway was affected in $Gilz^{-/-}$ mice. As shown in Fig. 6, SPAK phosphorylation at S373 was significantly elevated in $Gilz^{-/-}$ mice relative to that in $Gilz^{+/+}$ mice without a concomitant change in total SPAK abundance. Total abundance of WNK1 and WNK4 was unchanged between $Gilz^{-/-}$ and $Gilz^{+/+}$ mice. These results are consistent with a role for NCC hyperactivation in the rapid response to sodium restriction. We did not detect any changes in full length α-, β-, and γ-ENaC or the proteolytically cleaved fragment of α- and γ-ENaC (Fig. 6 and data not shown).

On the other hand, when we examined the phosphorylation of NCC at T53 and T58 in membrane fractions obtained from kidneys of mice fed a sodium deficient diet for 10 days, we saw no differences between $Gilz^{+/+}$ and $Gilz^{-/-}$ mice (Fig. 7). This was consistent with the fact that both $Gilz^{+/+}$ and $Gilz^{-/-}$ mice had reached steady state after 10 days of sodium restriction and the hypernatremia observed in $Gilz^{-/-}$ mice after 16 h of sodium restriction was corrected at this time. However, the phosphorylated SPAK/OSR1, total WNK1 and WNK4 levels were elevated in $Gilz^{-/-}$ mice compared to the $Gilz^{+/+}$ mice after 10 days of sodium restriction (Fig 7). Surprisingly, despite the frank hyperkalemia displayed by the

Gilz$^{-/-}$ mice at 10 day, we did not detect any changes in full length α-, β-, and γ-ENaC or the proteolytically cleaved fragment of α- and γ-ENaC (Fig. 7).

Levels of ROMK and BK$_{ca}$ potassium channels in *Gilz*$^{-/-}$ mice

Potassium secretion in the distal nephron is mediated by at least two types of channels: the renal outer medullary K channel (ROMK) and the large Ca^{2+}-activated K channel (BK$_{ca}$). We assessed the expression of ROMK and BK$_{ca}$ - α and β4 subunits in membrane preparations from kidneys of *Gilz*$^{-/-}$ and wild type littermates. Despite the mild elevation in plasma [K$^+$], there was no significant difference in the membrane expression of ROMK or BK$_{ca}$- α and β4 subunits between *Gilz*$^{-+/+}$ and *Gilz*$^{-/-}$ mice maintained on normal Na$^+$ diet, (Fig. 8A). After 16 h of Na$^+$ deprivation, ROMK and BK$_{ca}$- β4 levels remained unchanged between *Gilz*$^{-/-}$ and *Gilz*$^{-+/+}$ mice, however, BK$_{ca}$- α abundance was significantly higher in *Gilz*$^{-/-}$ mice than the *Gilz*$^{-+/+}$ mice (Fig. 8B). This difference had resolved by 10 days of low Na$^+$ diet, and neither ROMK nor BK$_{ca}$- α abundance in *Gilz*$^{-/-}$ mice was different from *Gilz*$^{-+/+}$ (Fig. 8C).

GILZ1 acts through WNK1 and SPAK/OSR1 to inhibit NCC surface expression and activation in cultured cells

Our *in vivo* experiments strongly supported a role for GILZ in inhibiting NCC. In order to explore the mechanism behind GILZ mediated NCC inhibition, we examined the effects of GILZ1 on NCC and its regulatory WNK-SPAK/OSR1 pathway in cultured cells. We first used surface biotinylation assays to capture plasma membrane NCC in HEK293T cells in the presence/absence of GILZ1 or another GILZ splice variant, GILZ2. Consistent with the *in vivo* results we found that GILZ1 but not GILZ2 inhibited cell surface NCC expression (Fig. 9). The total NCC expression in whole cell extract remained unchanged. We next examined the effect of GILZ1 on NCC phosphorylation in response to hypotonic low-Cl$^-$ treatment, which has been shown to induce phosphorylation and activation of WNK isoforms.[27, 33] Subsequently active WNKs phosphorylate and activate the related protein kinases SPAK and OSR1. Previous studies revealed that WNK1 kinase activity and SPAK/OSR1 phosphorylation are increased within 5 min of incubation in hypotonic low Cl$^-$ conditions, and NCC phosphorylation is increased after 10 min and reaches its maximum at 20–30min.[27, 33] We found similarly that hypotonic low-Cl$^-$ treatment for 30 min stimulated NCC phosphorylation in HEK293T cells (Fig. 10). We further found that this stimulation was markedly inhibited by expression of GILZ1 in a dose dependent manner although there was no significant change in total NCC expression level (Fig. 10). As mentioned above NCC phosphorylation is increased in patients with higher WNK1 or WNK4 levels. Hence, we looked at WNK4 levels in HEK293T cells treated with either control or hypotonic low Cl$^-$ buffer in the presence of increasing amounts of GILZ1. We did not see any changes in WNK4 levels in cells treated with either control or hypotonic low Cl$^-$ buffer due to GILZ1 co-expression (Fig. 11A). WNK1 levels were also unchanged in GILZ1 expressing cells when treated with control buffer as well as hypotonic low Cl$^-$ buffer (Fig. 11B). However, due to the low expression of WNK1 and high variability between experiments, the result for hypotonic low Cl$^-$ treatment was not as robust.

To examine if the WNK-SPAK/OSR1 pathway played a role in GILZ1 mediated inhibition of NCC, we examined the effects of GILZ1 on NCC activation in the presence of wild type SPAK (SPAK.WT), constitutively active $^{T243E/S383D}$SPAK (SPAK.CA), or kinase dead ^{K104R}SPAK (SPAK.KD). As shown in Fig. 12A, GILZ1 inhibited NCC phosphorylation in the presence of heterologously expressed wild type SPAK, but not constitutively active SPAK. Additionally, in the presence of kinase dead SPAK, NCC phosphorylation was almost completely abolished (Fig. 12A, compare lanes1 and 6), as previously described.[27] Together, these findings provide strong support for the idea that GILZ1 inhibits NCC by inhibiting SPAK activation.

To further elucidate the mechanism of GILZ1 mediated regulation of NCC; we overexpressed wild type Myc-tagged SPAK in HEK293T cells and stimulated the WNK-SPAK/OSR1 pathway by exposing the cells to hypotonic low-Cl$^-$ buffer. As expected, hypotonic low-Cl$^-$ stimulated the phosphorylation of SPAK at S373.[34] Increasing amounts of GILZ1 inhibited SPAK phosphorylation in a dose dependent manner (Fig. 12B). These results show that GILZ1 inhibits cell surface expression of NCC as well its activation in response to hypotonic low-Cl$^-$ treatment and this inhibition is at least in part achieved by GILZ1 mediated inhibition of SPAK phosphorylation and activation.

Discussion

Potassium homeostasis is maintained by K$^+$ secretion in the connecting tubule and cortical collecting duct via ROMK and BK$_{ca}$ channels along a favorable electrochemical gradient created by ENaC-mediated electrogenic Na$^+$ reabsorption. During dietary Na$^+$ restriction, multiple mechanisms act to increase Na$^+$ reabsorption in the kidney tubules by NCC as well as ENaC.[35] However, avid electroneutral Na$^+$ reabsorption by NCC can limit K$^+$ secretion by limiting Na$^+$ delivery to ENaC, and lead to elevation in plasma [K$^+$].[11, 36] Aldosterone plays a central role in the hormonal response to low dietary Na$^+$. One of its main roles is to defend the body from hyperkalemia by stimulating electrogenic Na$^+$ reabsorption, and thereby favoring K$^+$ secretion. *Gilz* was initially identified as a glucocorticoid-stimulated gene in immune cells,[13] but was later found to respond to aldosterone and to stimulate ENaC *in vitro*.[15, 37] Since then, the characterization of two strains of *Gilz$^{-/-}$* mice have revealed abnormalities in electrolyte balance but not the Na$^+$ wasting predicted on the basis of *in vitro* studies focusing solely on ENaC.[18, 19] In the present study, we show that this discrepancy is at least in part due to a role of GILZ as a negative regulator of NCC.

Our present data suggest that GILZ contributes to K$^+$ homeostasis by limiting NCC mediated electroneutral Na$^+$ reabsorption and promoting ENaC. Indeed, mice lacking GILZ adapt to sodium restriction *more* rapidly than do wild type mice. Additionally, *Gilz$^{-/-}$* mice are more sensitive to inhibition of NCC (HCTZ) but not ENaC (benzamil). The NCC hyperactivation appears to influence plasma [K$^+$] in that *Gilz$^{-/-}$* mice have higher [K$^+$] than *Gilz$^{+/+}$*, even at baseline, and become frankly hyperkalemic on sodium restricted diet. These results support the idea that hyperactivation of NCC is the predominant contributor to the enhanced response to Na$^+$ restriction in *Gilz$^{-/-}$* mice. Therefore, our results strongly suggest a role for GILZ in sustaining Na$^+$ delivery to ENaC-expressing nephron segments through NCC inhibition and thereby preventing hyperkalemia. Recent evidence supports the idea that

plasma $[K^+]$ itself can act through WNK kinases to inhibit NCC activity locally in the distal nephron,[38, 39] However, in the absence of GILZ, a greater rise in plasma $[K^+]$ is required to achieve this inhibition. It will be of considerable interest to determine if the effect of GILZ1 on NCC can be influenced by factors other than aldosterone, which would provide greater context-dependence to its NCC inhibitory effects.

Interestingly, despite the hyperstimulation of NCC, $Gilz^{-/-}$ mice had similar BP to that of the $Gilz^{+/+}$ mice. It is possible that the development of hypertension in these mice is age dependent (we have looked at young mice of 8–10 weeks of age), similar to FHHt patients. Notably, less than 20% of patients carrying an FHHt mutation develop hypertension before the age of 18 except those with Cullin 3 mutations.[40] Another possibility is that there are compensations in the $Gilz^{-/-}$ mice that prevent the development of hypertension but are unable to fully compensate for the impaired renal K^+ excretion. Along these lines, it is interesting to note that abundant *in vitro* data support the role of GILZ in stimulating ENaC. [37] It is possible that a mild defect in ENaC in the $Gilz^{-/-}$ mice leaves the animals normotensive yet hyperkalemic, but the phenotype is not sufficiently robust to be detected in our study (see below).

It should be emphasized that the mild elevation in plasma $[Na^+]$ observed in $Gilz^{-/-}$ mice is unlikely to be caused by defects in water handling, since both $Gilz^{+/+}$ and $Gilz^{-/-}$ display indistinguishable responses to water restriction (PR, unpublished results, and Suarez et al. [18]). Mild hypernatremia is typical of hypernatriferic states.[41, 42] We also did not observe differences in water or food consumption between $Gilz^{+/+}$ and $Gilz^{-/-}$ mice, nor did we observe any difference in their aldosterone levels. However, we did find a distinct difference in the acute PRA response to Na^+ restriction: 16 h of sodium restriction resulted in significantly increased PRA in $Gilz^{+/+}$ mice but not in $Gilz^{-/-}$ mice. This observation is consistent with higher baseline NCC activity in $Gilz^{-/-}$ mice. We believe that aldosterone secretion in $Gilz^{-/-}$ mice is more dependent on plasma $[K^+]$, as was observed in $WNK4^{D561A/+}$ knock in mice.[22] It is unclear why we did not see a significant difference in PRA between $Gilz^{+/+}$ and $Gilz^{-/-}$ mice under steady state conditions, as reported by Yang et al.[22]. It is possible that there are adaptations in the $Gilz^{-/-}$ mice not found in $WNK4^{D561A/+}$. It is also possible that a difference in PRA was not observed for technical reasons, as the $WNK4^{D561A/+}$ knock-in mice have a more marked phenotype than do the $Gilz^{-/-}$ mice.

In contrast to NCC, we did not observe any difference in ENaC expression as well as sensitivity towards the ENaC inhibitor benzamil between $Gilz^{+/+}$ and $Gilz^{-/-}$ mice. These observations are surprising in light of previously published *in vitro* studies showing that GILZ1 stimulates ENaC mediated Na^+-transport.[15] There are several possible explanations for this discrepancy: 1) Differences in ENaC activity are only detectable at earlier time points of low-Na^+ diet which we were not able to assess; 2) Compensatory effects may override a defect in ENaC activation as seen in SGK1 knockout mice.[43] Interestingly, a recent study by Loh et al. showed that sub-chronic testosterone treatment in orchidectomized rats causes elevated ENaC α, β, and γ mRNA and protein expression.[44] It is possible that the independent effect of testosterone on ENaC masks the inhibitory effects of *Gilz* deletion in whole body; 3) The effects of GILZ1 observed *in vitro* are not manifested *in vivo*. Additional studies will be necessary to distinguish these possibilities. We also did not

observe any changes in ROMK, BK_{ca} - subunits α and β4 between $Gilz^{-/-}$ mice and wild type littermates either at baseline or after prolonged Na^+ deprivation. However, we did see a significantly higher membrane expression of BK_{ca} - α subunit after 16h of Na^+ deprivation in $Gilz^{-/-}$ mice compared to $Gilz^{+/+}$. Based on previous studies suggesting a role for BK_{ca} - α in maintaining K^+ secretion during reduced Na^+ supplies[45], we believe that the observed increase in BK_{ca} - α in $Gilz^{-/-}$ mice is an adaptive response to high plasma $[K^+]$ in the face of Na^+ restriction. Upon prolonged Na^+ restriction $Gilz^{+/+}$ mice reach the same level of BK_{ca} - α stimulation. Though, it should be noted that the lack of any changes in either ENaC or ROMK or BK_{ca} levels in our study could also be due to the fact that the abundance of proteins in total membrane fractions might not accurately represent events occurring at the plasma membrane. Hence, it is possible that we are unable to see changes in these proteins due to technical limitations.

To our knowledge, this study is the first to show GILZ mediated regulation of plasma $[K^+]$, especially in the context of prolonged Na^+ restriction. These results might have important clinical implications as patients with various hypernatriferic states, including salt sensitive hypertension and congestive heart failure are frequently advised to restrict their dietary salt. It will be interesting to further investigate if there are GILZ polymorphisms that might cause a subset of these patients to be more susceptible to the development of hyperkalemia.

Our *in vitro* results also provide a first step in characterizing the mechanisms by which GILZ1 modulates NCC activity. In HEK293T cells, surface expression of NCC is lower in the presence of exogenously expressed GILZ1 but not its close relative GILZ2. GILZ1 also inhibits NCC phosphorylation at the key activating residues (T53 and T58) in response to hypotonic low Cl^- treatment. Furthermore, GILZ1 mediated NCC inhibition is at least in part due to reduced SPAK dependent NCC phosphorylation since NCC is insensitive to GILZ1 in the presence of constitutively active SPAK. Additionally, we did not see any effect of GILZ1 on WNK1 or WNK4 levels in either non-stimulated or hypotonic low Cl^- treated cells. These results are consistent with the *in vivo* results in that short term Na^+ deprivation led to greater NCC and SPAK phosphorylation in $Gilz^{-/-}$ mice than in $Gilz^{+/+}$ mice, without any change in WNK1 or WNK4 expression. In contrast, prolonged Na^+ deprivation (10 days of low Na^+ diet) did lead to significantly higher WNK1 and WNK4 levels in $Gilz^{-/-}$ mice than in $Gilz^{+/+}$. The reason for this increase is unclear, however, we speculate that it is not a direct effect of GILZ. We believe that after prolonged Na^+ restriction, there are multiple additional mechanisms, which are absent early on or in an *in vitro* model such as HEK293 cells. It should be noted that SPAK phosphorylation is inhibited by GILZ following short term as well as prolonged Na^+ restriction. Taken together, our *in vivo* and *in vitro* data strongly suggest that a central effect of GILZ1 is to inhibit SPAK phosphorylation, leading to decreased NCC phosphorylation at T53 and T58 with a concomitant decrease in active NCC at the plasma membrane. It does not appear that this effect of GILZ1 is due to a reduction in WNK1 or WNK4 levels, but rather to a decrease in their ability to phosphorylate and activate SPAK.

The schematic shown in Fig. 13 suggests a model for the role of GILZ in the coordinated regulation of Na^+ and K^+ handling by the distal nephron. On a normal Na^+ diet, NCC, ENaC and ROMK (for simplicity, all the transporters have been shown in the same cell) are in their

basal state in $Gilz^{+/+}$ mice (upper panels). Despite low aldosterone levels, some GILZ1 is expressed, which plays a role in maintaining baseline plasma [K$^+$] (4.3mM). After a short interval of Na$^+$ deprivation (16h), the renin angiotensin aldosterone system and other natriferic systems are activated, stimulating a variety of Na$^+$ transporters, in proximal convoluted tubule (particularly NHE3), thick ascending limb (NKCC2), DCT (NCC) and collecting duct (ENaC). Due to the stimulation of the more proximal Na$^+$ transporters, Na$^+$ delivery to ENaC-expressing segments decreases and plasma [K$^+$] rises slightly (from 4.3 to 4.6mM). The aldosterone-induced increase in GILZ1 blunts the rise in plasma [K$^+$] by inhibiting NCC, and possibly stimulating ENaC.[37] In the absence of GILZ1 (lower panels), baseline plasma [K$^+$] is already higher than in Gilz$^{+/+}$ (4.9 vs. 4.3mM). The elevated plasma [K$^+$] causes WNK4 inhibition as previously described.[39] During Na$^+$ deprivation, the direct inhibitory effect of elevated plasma [K$^+$] is initially sufficient to prevent a further rise in plasma [K$^+$]. However, as the mice become increasingly hypernatriferic, plasma [K$^+$] further rises resulting in frank hyperkalemia (5.2mM). Note that the plasma [K$^+$] is higher in $Gilz^{-/-}$ mice in all cases (normal salt diet, short term Na$^+$ deprivation, and long term Na$^+$ deprivation). We believe that the response of the WNK4-SPAK signaling module to elevated plasma [K$^+$] is intact in $Gilz^{-/-}$ mice, but it is right-shifted: i.e., higher levels of plasma [K$^+$] are required to inhibit WNK4/SPAK activation of NCC. When plasma [K$^+$] is elevated, transmembrane potential is reduced, resulting in Cl$^-$ entry into the cell, which inhibits WNK4 through direct physical interaction.[38] We propose that GILZ1 augments the ability of Cl$^-$ to inhibit WNK4, possibly by enhancing the interaction of Cl$^-$ with the kinase, or by enhancing the Cl$^-$ induced conformational change in WNK4. This leads to NCC inhibition, increased distal delivery of Na$^+$, greater ENaC mediated Na$^+$ reabsorption and augmented ROMK and/or BK$_{ca}$-mediated K$^+$ secretion (not shown in the model for simplicity).

Materials and Methods

Animals

All animals were housed in a controlled environment with a 12-h light and 12-h dark cycle with free access to water and a standard laboratory diet. All animal experiments were conducted under the approval of UCSF Institutional Animal Care and Usage Committee.

Generation of null mutant *Tsc22d-3* mice

The mouse *Tsc22d-3/Gilz* gene is located on chromosome X and contains six exons that result in multiple transcripts.[14] Generation of *Gilz* null mice was carried out in collaboration with geneOway. The targeting strategy designed led to the deletion of the exons 3 and 4, resulting in a *Gilz* constitutive knockout allele. Since *Gilz*$^{-/-}$ males are sterile, we were unable to obtain homozygous females and used hemizygous males for our experiments. The control group consisted of age-matched *Tsc22d3-2*$^{+/y}$ and *Tsc22d3-2*$^{lox/y}$ littermates. Genotyping was performed by PCR analysis of genomic DNA isolated from tail snips of newborn mice. Detailed targeting strategy and validation of the *Gilz*$^{-/-}$ mouse has been provided in supplemental experimental procedures and further information is available upon request.

Balance cage studies

Mice (8–12 week old) were acclimated to balance cages (Techniplast) for 3 days. A powder diet containing 0.49% NaCl (normal salt) was provided, and switched to salt-deficient diet (0.01% NaCl, Harlan Laboratories) as indicated. Urine was collected under water-saturated light mineral oil and stored at 4°C until analysis. Samples were sent to Stanford University Department of Comparative medicine Diagnostic Laboratory for urinary electrolyte measurements. After urine collection, whole blood was collected via retro-orbital bleeding (under anesthesia) and placed into heparinized Eppendorf tubes. 90 μl of whole blood was immediately added to a Chem8+ cartridge and analyzed using i-STAT analyzer (Abbot Point of Care Inc.). Rest of whole blood was centrifuged, plasma was collected and stored at −80°C until further analysis. Animals were sacrificed and kidneys were collected for Western blot analysis.

Blood Pressure Measurement

BP was measured non-invasively in conscious mice by determining the tail blood volume with a volume-pressure recording (VPR) sensor and an occlusion tail-cuff using a computerized system (CODA noninvasive BP system, Kent Scientific, Torrington, CT). Data was collected for three consecutive days from 8–10 week old mice and mean values were used as the final BP reading.

Aldosterone and Plasma renin Activity

Urinary aldosterone levels were measured by ELISA (IBL-America). PRA was measured as the amount of angiotensin I generated after incubation with excess angiotensinogen (Sigma). Two microliters of plasma were incubated with excess porcine angiotensinogen (4 μM) in a reaction containing sodium acetate (50 mM, pH 6.5), AEBSF (2.5 mM), 8-hydroxyquinoline (1 mM), and EDTA (5 mM) for 15 min at 37°C. The assay was linear for at least 30 min. The reaction was stopped by boiling for 5 min and angiotensin I was measured by ELISA (Phoenix Pharmaceuticals).

Natriuretic experiments

Mice (8–12 week old) were placed in balance cages and acclimated for 3 days. All drugs were prepared in sterile saline solution containing 20% DMSO and 40% polyethylene glycol (PEG); vehicle solution contained saline with 20% DMSO and 40% PEG. Animals were injected (IP) with vehicle, thiazide (25 mg/kg body weight) or benzamil (1.5 mg/kg body weight) and urine was collected for 6 h.

Preparation of kidney cytosolic and total membrane extracts

Mice were placed on either normal or low-Na$^+$ diet. For low-Na$^+$ diet experiments, kidneys were excised after 16 h or 10 day of low Na$^+$ diet and snap-frozen in liquid nitrogen. Frozen kidneys were homogenized by crushing with a mortar and pestle on dry ice. Membrane Fractionation kit (Biovision) was used to enrich the cytosolic and crude membrane protein fractions according to the manufacturer's protocol. 50–100 μg cytosolic fraction or crude membrane fraction protein was run on SDS-PAGE and transferred to PVDF membrane for immunoblotting. Antibodies against various proteins were obtained as follows: anti–Pan

Cadherin (Cell Signaling); anti–N-terminal αENaC, βENaC, γENaC, ROMK (gifts from J. Loffing, University of Zurich, Zurich, Switzerland); anti-phospho-NCC T53, anti-WNK1/4 (gifts from D. Ellison, Oregon Health & Science University, Oregon, USA); anti–phospho-NCC T58, anti-phospho-NCC T53/58 and anti-NCC (gifts from R. Fenton, Aarhus University, Denmark, Sweden); anti-phospo SPAK (Millipore), anti-total SPAK (Millipore); anti-BK$_{ca}$- α and β4 (Alomone Labs).

Hypotonic treatment of HEK293T cells

HEK293T cells were regularly maintained in plastic tissue culture flasks at 37 °C in DMEM supplemented with 10% fetal bovine serum and 100 units/ml penicillin/streptomycin. Cells were grown to 60–70% confluence and transfected as indicated using PEI. 48 h after transfection, cells were washed and incubated in either control basic buffer or hypotonic buffer for desired times.

Basic buffer was 135 mM NaCl, 5 mM KCl, 0.5 mM CaCl$_2$, 0.5 mM MgCl$_2$, 0.5 mM Na$_2$HPO$_4$, 0.5 mM Na$_2$SO$_4$ and 15 mM HEPES. Hypotonic low-chloride buffer was 67.5 mM Na gluconate, 2.5 mM K gluconate, 0.25 mM CaCl$_2$, 0.25 mM MgCl$_2$, 0.5 mM Na$_2$HPO$_4$, 0.5 mM Na$_2$SO$_4$ and 7.5 mM HEPES.

Cell Surface Biotinylation Assays

HEK293T cells were transfected as specified. Forty-eight hours after transfection, cells were treated with EZ-Link Sulfo-NHS-Biotin (Thermo Scientific) for 1 h before extraction and recovery of biotinylated proteins with immobilized neutravidin beads (Thermo Scientific). Immunoprecipitates were analyzed for cell surface (biotinylated) proteins. Total GAPDH was used as a loading control for cytoplasmic fraction while Pan-cadherin was used as loading control for plasma membrane fraction.

Immunoprecipitation and Western Blots

Cell lysates were prepared after 48 h of transfection and immunoprecipitation was performed using Flag-conjugated sepharose beads (Sigma). Immunoblotting was done using our anti-GILZ antibody, anti-Flag-HRP antibody (Sigma), anti-HA-HRP antibody (Roche), and anti-Myc (Cell Signaling) antibodies. Each experiment was repeated at least three times independently with similar results.

Statistical Analysis

For densitometric analysis of immunoblots, signal intensities of specified bands were determined using NIH ImageJ software and normalized to that of the internal control. Values so obtained were used to determine mean ± S.E.M for a graphical representation. For tissue samples, we excluded any bands with intensity lower than that of the background and the corresponding animals were removed from the analysis. For balance studies with *Gilz*$^{+/+}$ or *Gilz*$^{-/-}$ mice and quantification of Western blots, statistical comparisons between groups were carried out using unpaired, 2-tailed Student's *t* test except where indicated otherwise. For all comparisons, a p-value less than 0.05 were considered statistically significant.

Supplementary Material

Refer to Web version on PubMed Central for supplementary material.

Acknowledgments

References

1. Meneton P, Loffing J, Warnock DG. Sodium and potassium handling by the aldosterone-sensitive distal nephron: the pivotal role of the distal and connecting tubule. American journal of physiology Renal physiology. 2004; 287:F593–601. [PubMed: 15345493]

2. Traslavina RP, King EJ, Loar AS, Riedel ER, Garvey MS, Ricart-Arbona R, Wolf FR, Couto SS. Euthanasia by CO(2) inhalation affects potassium levels in mice. Journal of the American Association for Laboratory Animal Science : JAALAS. 2010; 49:316–322. [PubMed: 20587163]

3. Stanton, BA., Giebisch, GH. Comprehensive Physiology. John Wiley & Sons, Inc.; 2010. Renal Potassium Transport.

4. Lifton RP, Gharavi AG, Geller DS. Molecular mechanisms of human hypertension. Cell. 2001; 104:545–556. [PubMed: 11239411]

5. Bhargava A, Wang J, Pearce D. Regulation of epithelial ion transport by aldosterone through changes in gene expression. Molecular and cellular endocrinology. 2004; 217:189–196. [PubMed: 15134817]

6. Soundararajan R, Pearce D, Ziera T. The role of the ENaC-regulatory complex in aldosterone-mediated sodium transport. Molecular and cellular endocrinology. 2012; 350:242–247. [PubMed: 22101317]

7. Giebisch G. Renal potassium transport: mechanisms and regulation. The American journal of physiology. 1998; 274:F817–833. [PubMed: 9612319]

8. Hoorn EJ, Loffing J, Ellison DH. An Integrated View of Potassium Homeostasis. The New England journal of medicine. 2015; 373:1786.

9. Wall SM, Weinstein AM. Cortical distal nephron Cl(−) transport in volume homeostasis and blood pressure regulation. American journal of physiology Renal physiology. 2013; 305:F427–438. [PubMed: 23637202]

10. Penton D, Czogalla J, Loffing J. Dietary potassium and the renal control of salt balance and blood pressure. Pflugers Archiv : European journal of physiology. 2015; 467:513–530. [PubMed: 25559844]

11. Hoorn EJ, Nelson JH, McCormick JA, Ellison DH. The WNK kinase network regulating sodium, potassium, and blood pressure. Journal of the American Society of Nephrology : JASN. 2011; 22:605–614. [PubMed: 21436285]

12. Rozansky DJ, Cornwall T, Subramanya AR, Rogers S, Yang YF, David LL, Zhu X, Yang CL, Ellison DH. Aldosterone mediates activation of the thiazide-sensitive Na-Cl cotransporter through an SGK1 and WNK4 signaling pathway. The Journal of clinical investigation. 2009; 119:2601–2612. [PubMed: 19690383]

13. D'Adamio F, Zollo O, Moraca R, Ayroldi E, Bruscoli S, Bartoli A, Cannarile L, Migliorati G, Riccardi C. A new dexamethasone-induced gene of the leucine zipper family protects T lymphocytes from TCR/CD3-activated cell death. Immunity. 1997; 7:803–812. [PubMed: 9430225]

14. Soundararajan R, Wang J, Melters D, Pearce D. Differential activities of glucocorticoid-induced leucine zipper protein isoforms. The Journal of biological chemistry. 2007; 282:36303–36313. [PubMed: 17956870]

15. Soundararajan R, Zhang TT, Wang J, Vandewalle A, Pearce D. A novel role for glucocorticoid-induced leucine zipper protein in epithelial sodium channel-mediated sodium transport. The Journal of biological chemistry. 2005; 280:39970–39981. [PubMed: 16216878]

16. Soundararajan R, Melters D, Shih IC, Wang J, Pearce D. Epithelial sodium channel regulated by differential composition of a signaling complex. Proceedings of the National Academy of Sciences of the United States of America. 2009; 106:7804–7809. [PubMed: 19380724]

17. Soundararajan R, Wang J, Melters D, Pearce D. Glucocorticoid-induced Leucine zipper 1 stimulates the epithelial sodium channel by regulating serum- and glucocorticoid-induced kinase 1 stability and subcellular localization. The Journal of biological chemistry. 2010; 285:39905–39913. [PubMed: 20947508]

18. Suarez PE, Rodriguez EG, Soundararajan R, Merillat AM, Stehle JC, Rotman S, Roger T, Voirol MJ, Wang J, Gross O, Petrilli V, Nadra K, Wilson A, Beermann F, Pralong FP, Maillard M, Pearce D, Chrast R, Rossier BC, Hummler E. The glucocorticoid-induced leucine zipper (gilz/Tsc22d3-2) gene locus plays a crucial role in male fertility. Molecular endocrinology. 2012; 26:1000–1013. [PubMed: 22556341]

19. Bruscoli S, Velardi E, Di Sante M, Bereshchenko O, Venanzi A, Coppo M, Berno V, Mameli MG, Colella R, Cavaliere A, Riccardi C. Long glucocorticoid-induced leucine zipper (L-GILZ) protein interacts with ras protein pathway and contributes to spermatogenesis control. The Journal of biological chemistry. 2012; 287:1242–1251. [PubMed: 22110132]

20. Bruscoli S, Biagioli M, Sorcini D, Frammartino T, Cimino M, Sportoletti P, Mazzon E, Bereshchenko O, Riccardi C. Lack of glucocorticoid-induced leucine zipper (GILZ) deregulates B-cell survival and results in B-cell lymphocytosis in mice. Blood. 2015; 126:1790–1801. [PubMed: 26276664]

21. Ayroldi E, Migliorati G, Bruscoli S, Marchetti C, Zollo O, Cannarile L, D'Adamio F, Riccardi C. Modulation of T-cell activation by the glucocorticoid-induced leucine zipper factor via inhibition of nuclear factor kappaB. Blood. 2001; 98:743–753. [PubMed: 11468175]

22. Yang SS, Morimoto T, Rai T, Chiga M, Sohara E, Ohno M, Uchida K, Lin SH, Moriguchi T, Shibuya H, Kondo Y, Sasaki S, Uchida S. Molecular pathogenesis of pseudohypoaldosteronism type II: generation and analysis of a Wnk4(D561A/+) knockin mouse model. Cell metabolism. 2007; 5:331–344. [PubMed: 17488636]

23. Yang SS, Fang YW, Tseng MH, Chu PY, Yu IS, Wu HC, Lin SW, Chau T, Uchida S, Sasaki S, Lin YF, Sytwu HK, Lin SH. Phosphorylation regulates NCC stability and transporter activity in vivo. Journal of the American Society of Nephrology : JASN. 2013; 24:1587–1597. [PubMed: 23833262]

24. Cantone A, Yang X, Yan Q, Giebisch G, Hebert SC, Wang T. Mouse model of type II Bartter's syndrome. I. Upregulation of thiazide-sensitive Na-Cl cotransport activity. American journal of physiology Renal physiology. 2008; 294:F1366–1372. [PubMed: 18385266]

25. Chiga M, Rai T, Yang SS, Ohta A, Takizawa T, Sasaki S, Uchida S. Dietary salt regulates the phosphorylation of OSR1/SPAK kinases and the sodium chloride cotransporter through aldosterone. Kidney international. 2008; 74:1403–1409. [PubMed: 18800028]

26. Yang SS, Lo YF, Wu CC, Lin SW, Yeh CJ, Chu P, Sytwu HK, Uchida S, Sasaki S, Lin SH. SPAK-knockout mice manifest Gitelman syndrome and impaired vasoconstriction. Journal of the American Society of Nephrology : JASN. 2010; 21:1868–1877. [PubMed: 20813865]

27. Richardson C, Rafiqi FH, Karlsson HK, Moleleki N, Vandewalle A, Campbell DG, Morrice NA, Alessi DR. Activation of the thiazide-sensitive Na+-Cl–cotransporter by the WNK-regulated kinases SPAK and OSR1. Journal of cell science. 2008; 121:675–684. [PubMed: 18270262]

28. Rafiqi FH, Zuber AM, Glover M, Richardson C, Fleming S, Jovanovic S, Jovanovic A, O'Shaughnessy KM, Alessi DR. Role of the WNK-activated SPAK kinase in regulating blood pressure. EMBO molecular medicine. 2010; 2:63–75. [PubMed: 20091762]

29. Mercier-Zuber A, O'Shaughnessy KM. Role of SPAK and OSR1 signalling in the regulation of NaCl cotransporters. Current opinion in nephrology and hypertension. 2011; 20:534–540. [PubMed: 21610494]

30. Wilson FH, Disse-Nicodeme S, Choate KA, Ishikawa K, Nelson-Williams C, Desitter I, Gunel M, Milford DV, Lipkin GW, Achard JM, Feely MP, Dussol B, Berland Y, Unwin RJ, Mayan H, Simon

DB, Farfel Z, Jeunemaitre X, Lifton RP. Human hypertension caused by mutations in WNK kinases. Science. 2001; 293:1107–1112. [PubMed: 11498583]

31. Terker AS, Yang CL, McCormick JA, Meermeier NP, Rogers SL, Grossmann S, Trompf K, Delpire E, Loffing J, Ellison DH. Sympathetic stimulation of thiazide-sensitive sodium chloride cotransport in the generation of salt-sensitive hypertension. Hypertension. 2014; 64:178–184. [PubMed: 24799612]

32. Castaneda-Bueno M, Gamba G. Mechanisms of sodium-chloride cotransporter modulation by angiotensin II. Current opinion in nephrology and hypertension. 2012; 21:516–522. [PubMed: 22820370]

33. Moriguchi T, Urushiyama S, Hisamoto N, Iemura S, Uchida S, Natsume T, Matsumoto K, Shibuya H. WNK1 regulates phosphorylation of cation-chloride-coupled cotransporters via the STE20-related kinases, SPAK and OSR1. The Journal of biological chemistry. 2005; 280:42685–42693. [PubMed: 16263722]

34. Vitari AC, Deak M, Morrice NA, Alessi DR. The WNK1 and WNK4 protein kinases that are mutated in Gordon's hypertension syndrome phosphorylate and activate SPAK and OSR1 protein kinases. The Biochemical journal. 2005; 391:17–24. [PubMed: 16083423]

35. Frindt G, Palmer LG. Surface expression of sodium channels and transporters in rat kidney: effects of dietary sodium. American journal of physiology Renal physiology. 2009; 297:F1249–1255. [PubMed: 19741015]

36. Glover M, O'Shaughnessy KM. Molecular insights from dysregulation of the thiazide-sensitive WNK/SPAK/NCC pathway in the kidney: Gordon syndrome and thiazide-induced hyponatraemia. Clinical and experimental pharmacology & physiology. 2013; 40:876–884. [PubMed: 23683032]

37. Pearce D, Soundararajan R, Trimpert C, Kashlan OB, Deen PM, Kohan DE. Collecting duct principal cell transport processes and their regulation. Clinical journal of the American Society of Nephrology : CJASN. 2015; 10:135–146. [PubMed: 24875192]

38. Terker AS, Zhang C, McCormick JA, Lazelle RA, Zhang C, Meermeier NP, Siler DA, Park HJ, Fu Y, Cohen DM, Weinstein AM, Wang WH, Yang CL, Ellison DH. Potassium modulates electrolyte balance and blood pressure through effects on distal cell voltage and chloride. Cell metabolism. 2015; 21:39–50. [PubMed: 25565204]

39. Terker AS, Zhang C, Erspamer KJ, Gamba G, Yang CL, Ellison DH. Unique chloride-sensing properties of WNK4 permit the distal nephron to modulate potassium homeostasis. Kidney international. 2015

40. Boyden LM, Choi M, Choate KA, Nelson-Williams CJ, Farhi A, Toka HR, Tikhonova IR, Bjornson R, Mane SM, Colussi G, Lebel M, Gordon RD, Semmekrot BA, Poujol A, Valimaki MJ, De Ferrari ME, Sanjad SA, Gutkin M, Karet FE, Tucci JR, Stockigt JR, Keppler-Noreuil KM, Porter CC, Anand SK, Whiteford ML, Davis ID, Dewar SB, Bettinelli A, Fadrowski JJ, Belsha CW, Hunley TE, Nelson RD, Trachtman H, Cole TR, Pinsk M, Bockenhauer D, Shenoy M, Vaidyanathan P, Foreman JW, Rasoulpour M, Thameem F, Al-Shahrouri HZ, Radhakrishnan J, Gharavi AG, Goilav B, Lifton RP. Mutations in kelch-like 3 and cullin 3 cause hypertension and electrolyte abnormalities. Nature. 2012; 482:98–102. [PubMed: 22266938]

41. Gregoire JR. Adjustment of the osmostat in primary aldosteronism. Mayo Clinic proceedings. 1994; 69:1108–1110. [PubMed: 7967766]

42. Eijgelsheim M, Hoorn EJ. Hypernatraemia: balancing is challenging. The Netherlands journal of medicine. 2015; 73:446–447. [PubMed: 26687259]

43. Wulff P, Vallon V, Huang DY, Volkl H, Yu F, Richter K, Jansen M, Schlunz M, Klingel K, Loffing J, Kauselmann G, Bosl MR, Lang F, Kuhl D. Impaired renal Na(+) retention in the sgk1-knockout mouse. The Journal of clinical investigation. 2002; 110:1263–1268. [PubMed: 12417564]

44. Loh SY, Giribabu N, Salleh N. Sub-chronic testosterone treatment increases the levels of epithelial sodium channel (ENaC)-alpha, beta and gamma in the kidney of orchidectomized adult male Sprague-Dawley rats. PeerJ. 2016; 4:e2145. [PubMed: 27413634]

45. Muto S, Tsuruoka S, Miyata Y, Fujimura A, Kusano E, Wang W, Seldin D, Giebisch G. Basolateral Na+/H+ exchange maintains potassium secretion during diminished sodium transport in the rabbit cortical collecting duct. Kidney international. 2009; 75:25–30. [PubMed: 18769367]
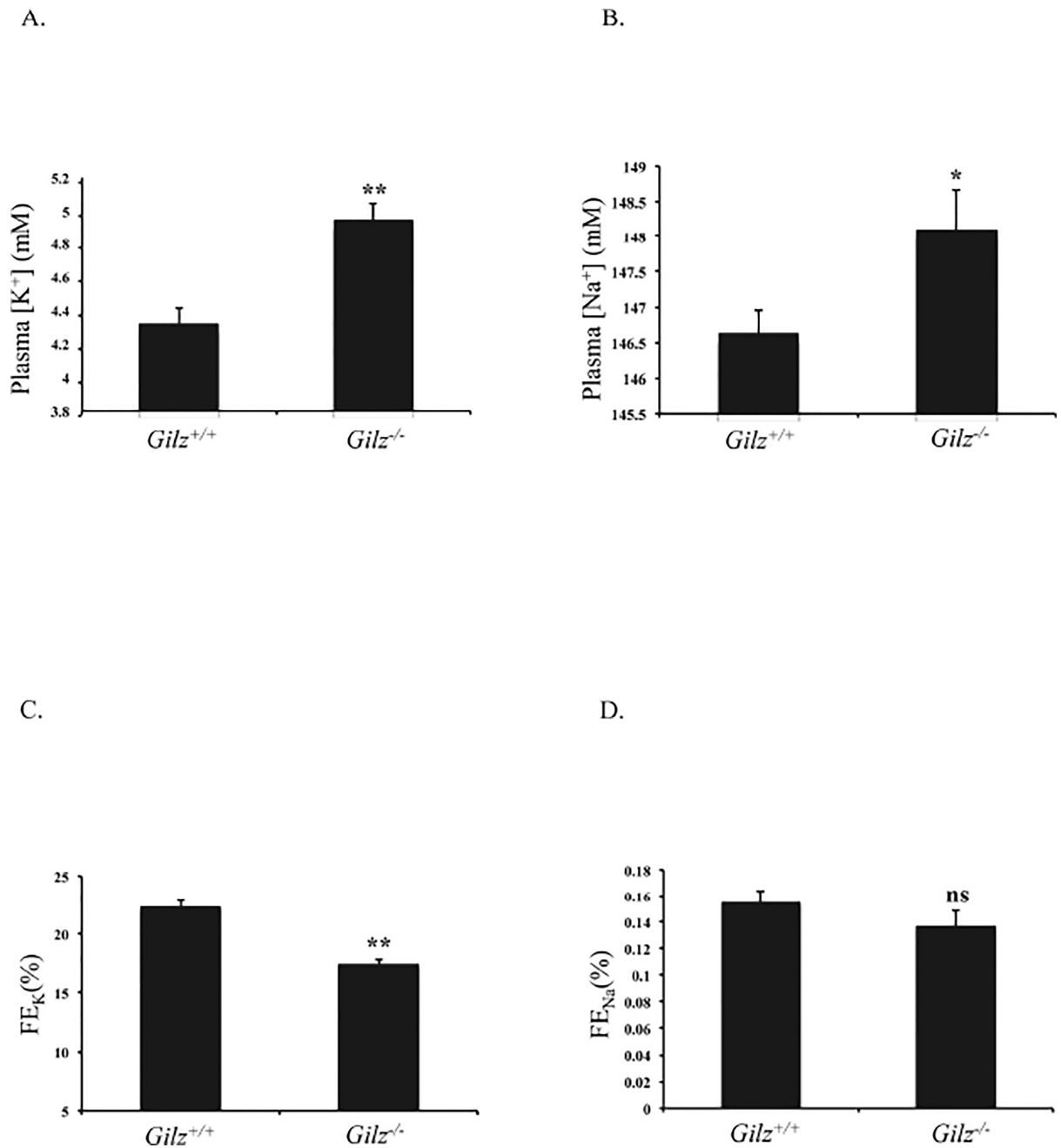
A.

B.

C.

D.

Figure 1. $Gilz^{-/-}$ mice maintained on normal Na^+ diet display abnormalities of plasma and urinary electrolytes

Mice (8 $Gilz^{+/+}$ and 10 $Gilz^{-/-}$) were maintained on normal Na^+ diet for three days in balance cages. Urine was collected for 16 h during dark cycle before blood collection. Blood and urinary electrolytes were measured as described in material and methods, and fractional excretion of K^+ (FE_K) and Na^+ (FE_{Na}) was calculated. (A) Plasma $[K^+]$; (B) Plasma $[Na^+]$; (C) FE_K and (D) FE_{Na}. Data represent mean ± SEM. p-value was calculated using bi-directional unpaired Student's t-test. *p-value<0.05 vs. $Gilz^{+/+}$; **p-value<0.001 vs. $Gilz^{+/+}$.
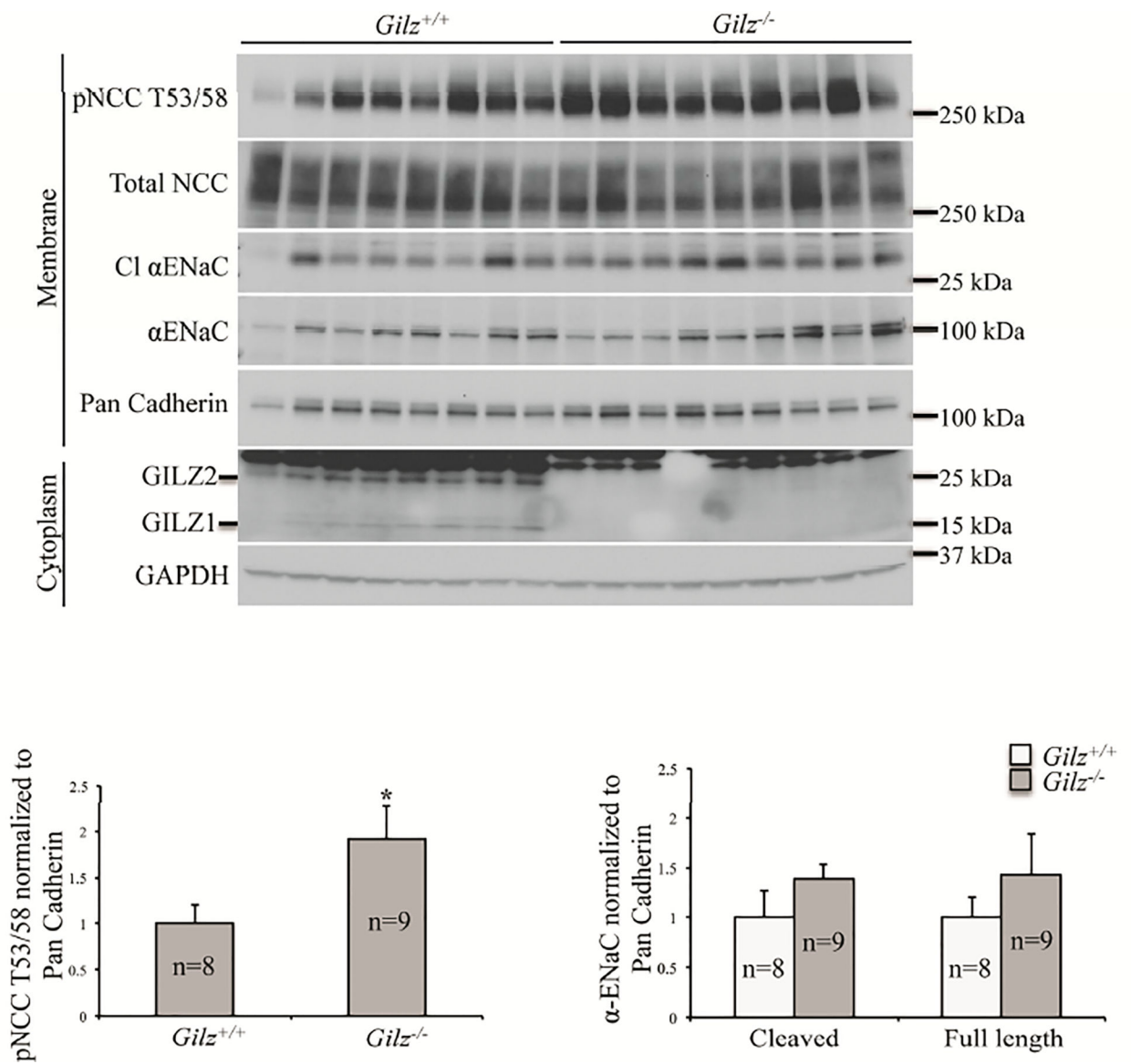
Figure 2. Expression of NCC (total and phosphorylated) and ENaC in kidneys of $Gilz^{+/+}$ and $Gilz^{-/-}$ mice maintained on normal Na$^+$ diet

Left kidneys obtained from mice described in Fig. 1 were used for membrane and cytosolic fraction enrichment using Biovision Membrane Extraction Kit (8 $Gilz^{+/+}$ and 9 $Gilz^{-/-}$ mice). Western blots were quantified by densitometry analysis. Data represent mean ± SEM. p-value was calculated using bi-directional unpaired Student's t-test. *p-value<0.05 vs. $Gilz^{+/+}$.

A. HCTZ
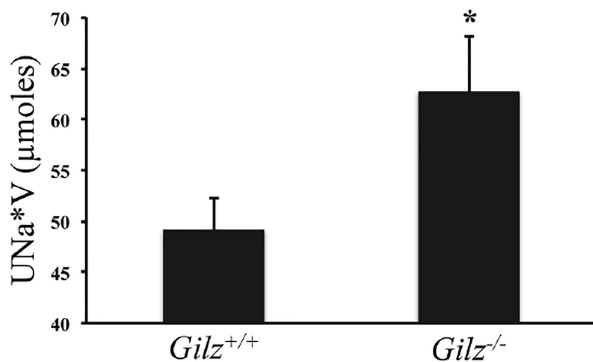
B. Benzamil
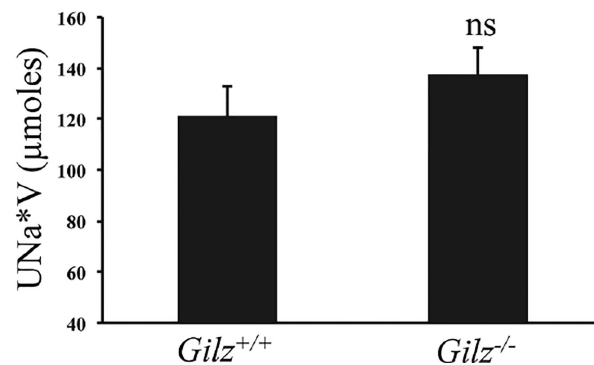
Figure 3. *Gilz*$^{-/-}$ mice are more sensitive to thiazide than *Gilz*$^{+/+}$

Gilz$^{+/+}$ and *Gilz*$^{-/-}$ mice were acclimatized for three days in balance cages on normal Na$^+$ diet. Mice were then treated with vehicle, thiazide (25mg/kg, 16 *Gilz*$^{+/+}$ and 12 *Gilz*$^{-/-}$ mice) or benzamil (1.5mg/kg, 9 *Gilz*$^{+/+}$ and 6 *Gilz*$^{-/-}$ mice) and urine was collected for six hours. Data represent mean ± SEM. p-value was calculated using bi-directional unpaired Student's t-test. *p-value<0.05 vs. *Gilz*$^{+/+}$. UNa*V: Total Na$^+$ (μmoles) excreted in the urine during 6 h of collection in response to (A) HCTZ; (B) Benzamil.

A.

B.

C.
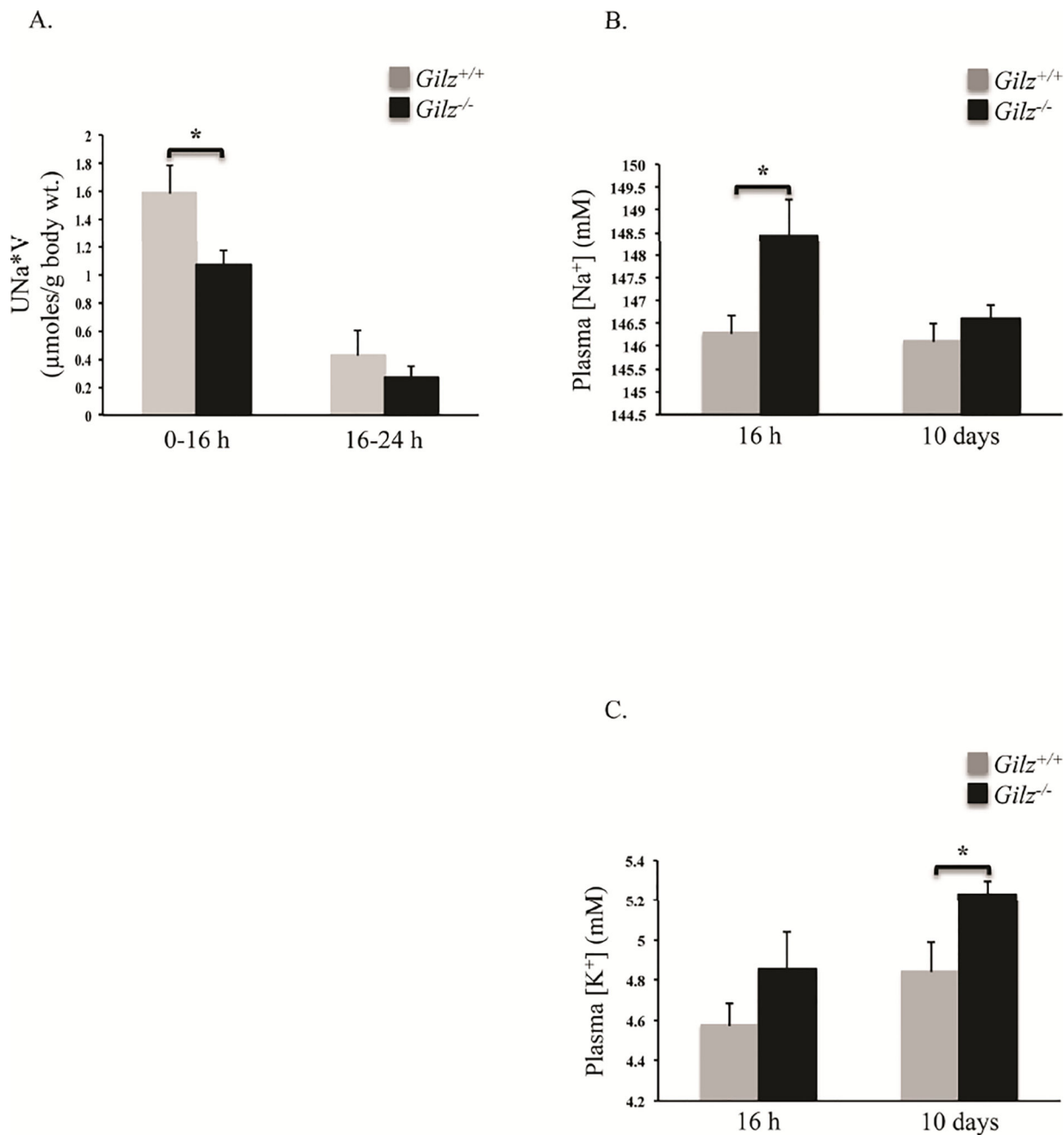
Figure 4. *Gilz*^{−/−} mice come into sodium balance more rapidly than the *Gilz*^{+/+} mice

Gilz^{+/+} and *Gilz*^{−/−} mice were acclimatized for three days in balance cages on normal Na^+ diet. The animals were then switched to low-Na^+ diet for either 16 h (20 *Gilz*^{+/+} and 20 *Gilz* [−/−] mice) or 10 days (8 *Gilz*^{+/+} and 8 *Gilz*^{−/−} mice). Data represent mean ± SEM. p-value was calculated using bi-directional unpaired Student's t-test. *p-value< 0.05 vs. *Gilz*^{+/+}.

A. Total Na^+ excreted in the urine (UNa*V) during the first 16 h and the next 8 h (data point represented as 16–24 h urinary Na^+ excretion).

B, C. After collecting urine, blood was collected using retro-orbital bleeding. Blood electrolytes were measured using i-STAT. B) Plasma [Na^+], C) Plasma [K^+].
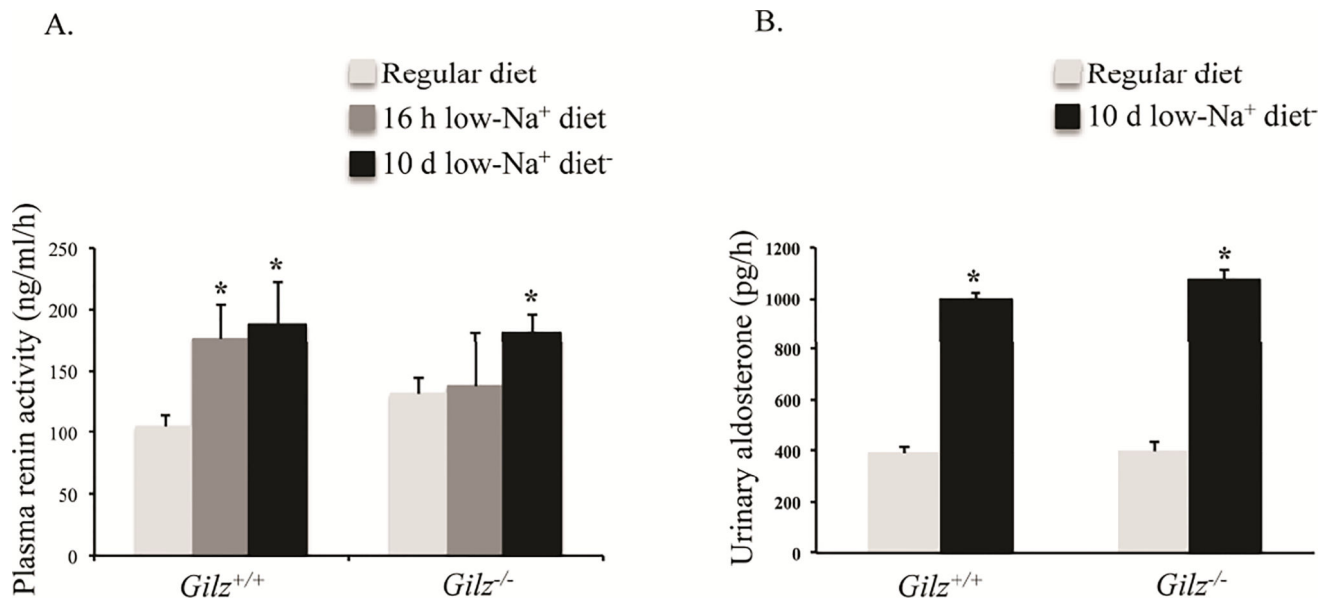
Figure 5. Plasma renin activity and aldosterone level in *Gilz*$^{-/-}$ mice

A. Blood was collected from mice maintained on normal Na$^+$ (8 *Gilz*$^{+/+}$ and 10 *Gilz*$^{-/-}$, described in Fig. 1) or low-Na$^+$ diet described in Fig. 4 for 16 h (20 *Gilz*$^{+/+}$ and 20 *Gilz*$^{-/-}$ mice) or 10 days (8 *Gilz*$^{+/+}$ and 8 *Gilz*$^{-/-}$ mice). Plasma renin activity was measured at indicated times as described in material and methods.

B. Basal urine as well as urine after 10 days on sodium deficient diet was collected (as described in Fig. 4) and total urinary aldosterone was measured by ELISA.

Data represent mean ± SEM. p-value was calculated using bi-directional unpaired Student's t-test within each genotype on normal Na$^+$ diet vs. sodium deficient diet as well as between the genotypes. *p-value < 0.05 compared to values on normal Na$^+$ diet within the genotype.
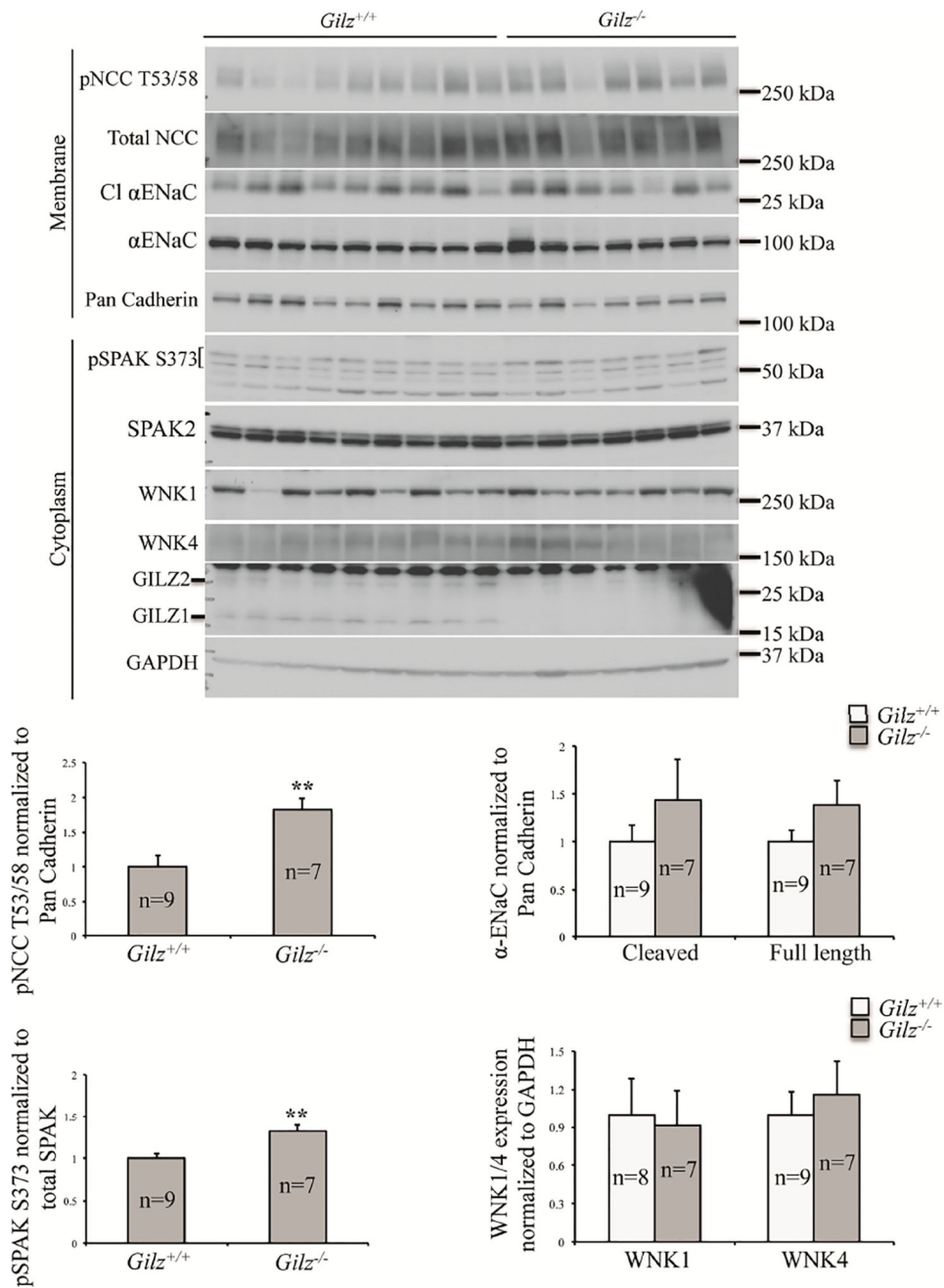
Figure 6. Expression of NCC (total and phosphorylated) and ENaC in kidneys of *Gilz*$^{+/+}$ and *Gilz*$^{-/-}$ mice maintained on low-Na$^+$ diet for 16 h

Kidneys were harvested from mice on a sodium deficient diet (0.01% NaCl) for 16 h (9 *Gilz*$^{+/+}$ and 7 *Gilz*$^{-/-}$ mice, described in Fig. 4) and left kidney was used for membrane and cytosolic fraction enrichment. Data represent mean ± SEM. p-value was calculated using bi-directional unpaired Student's t-test. **p-value<0.005 vs. *Gilz*$^{+/+}$.
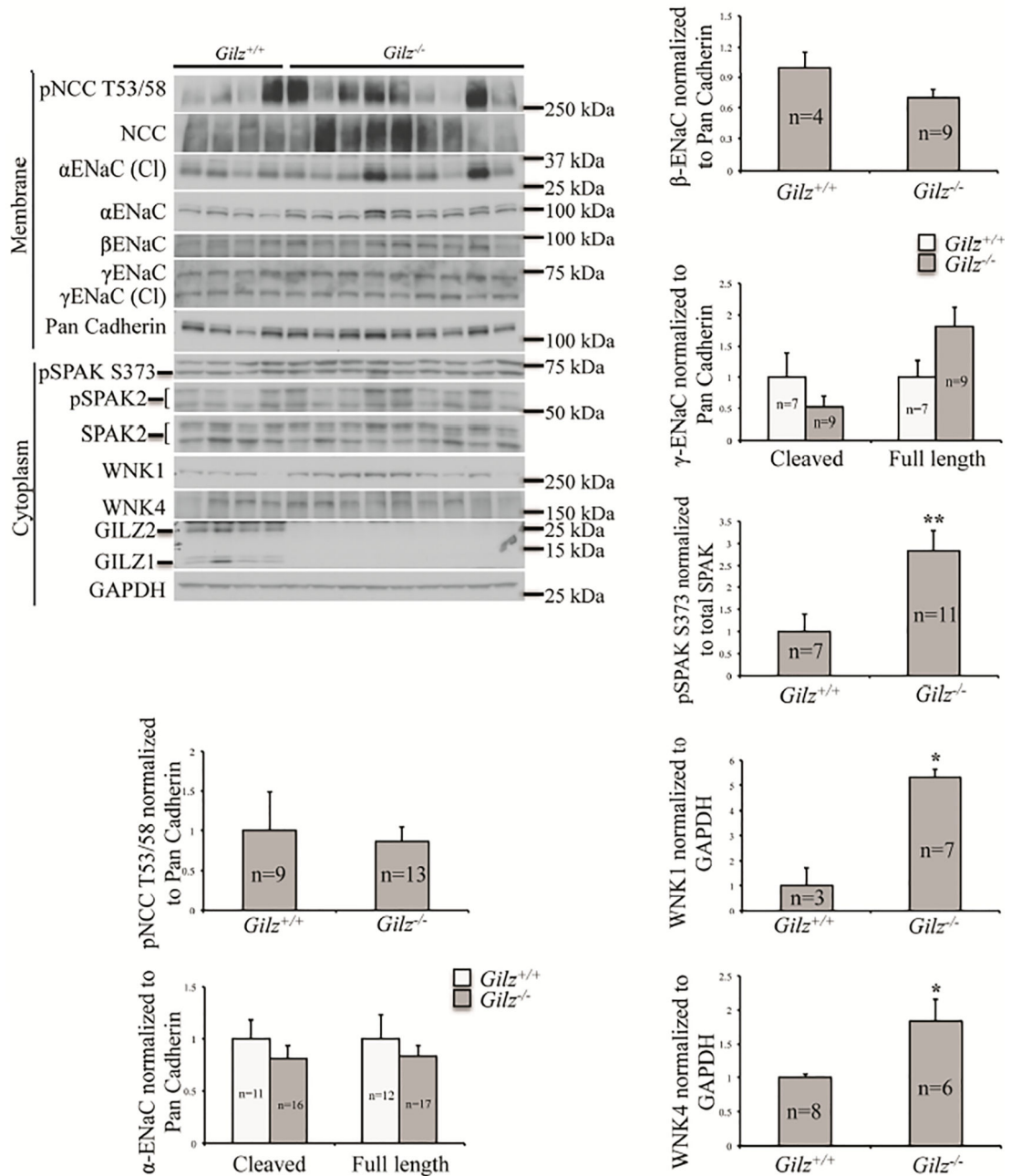
Figure 7. Expression of NCC (total and phosphorylated) and ENaC in kidneys of $Gilz^{+/+}$ and $Gilz^{-/-}$ mice maintained on low-Na$^+$ diet for 10 days

Mice (12 $Gilz^{+/+}$ and 17 $Gilz^{-/-}$) were acclimatized for three days in metabolic cages on normal Na$^+$ diet. Mice were then switched to a sodium deficient diet (0.01% NaCl) for 10 days. Kidneys were harvested and left kidney was used for membrane and cytosolic fraction enrichment. Data represent mean ± SEM. p-value was calculated using bi-directional unpaired Student's t-test. *p-value<0.05 vs. $Gilz^{+/+}$; **p-value<0.005 vs. $Gilz^{+/+}$.
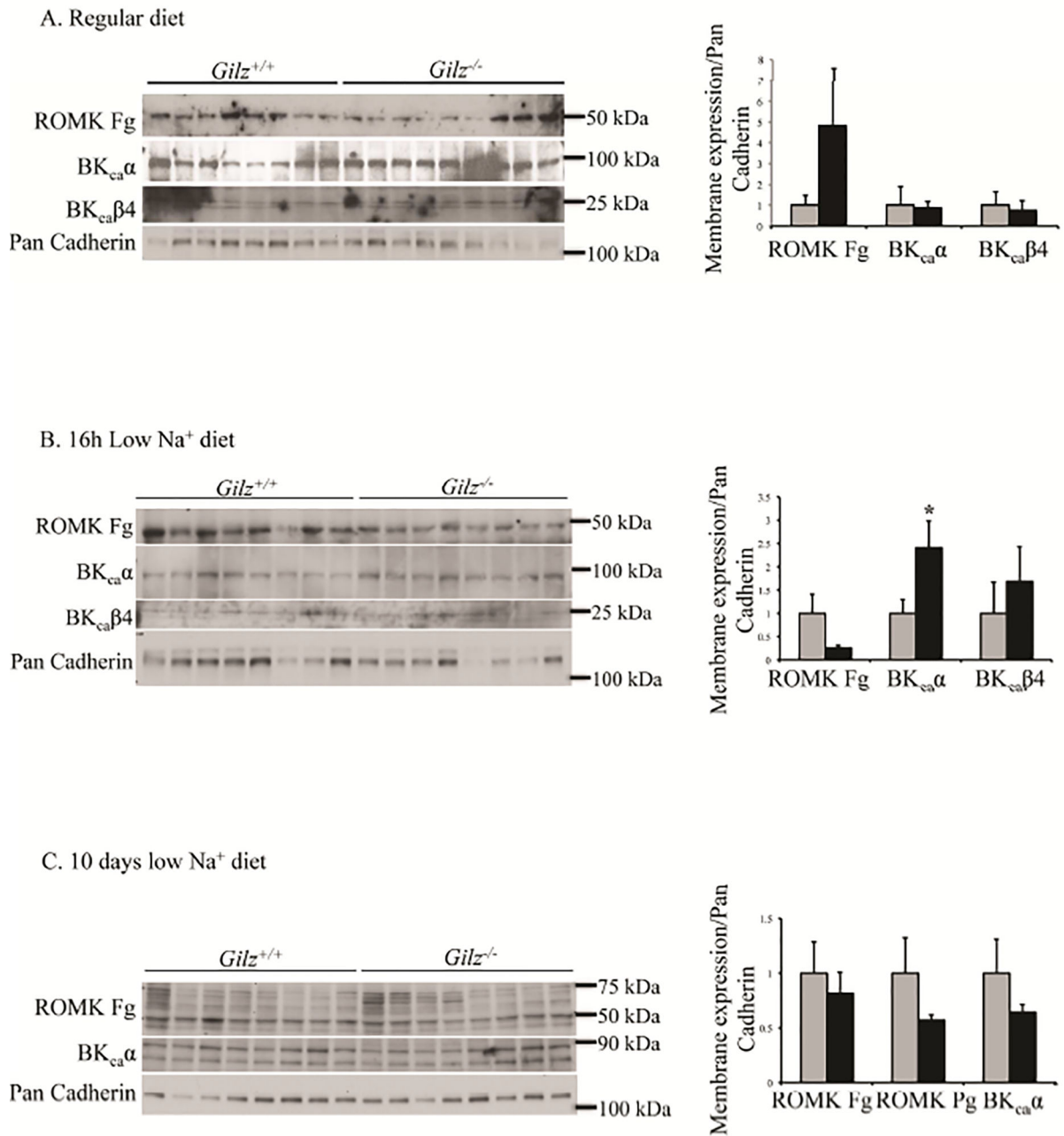
Figure 8. Expression of ROMK and BK$_{ca}$ channel in kidneys of *Gilz*$^{+/+}$ and *Gilz*$^{-/-}$ mice
Total membrane proteins and cytosolic fractions described in Fig. 2 (normal Na$^+$ diet), Fig. 6 (16 h low Na$^+$ diet) and Fig. 7 (10 days low Na$^+$ diet) were probed for indicated proteins. Fg: fully glycosylated, Pg: partially glycosylated. Western blots were quantified by densitometry analysis. Data represent mean ± SEM. p-value was calculated using bidirectional unpaired Student's t-test. *p-value<0.05 vs. *Gilz*$^{+/+}$. (A) Normal Na$^+$ diet; (B) Low Na$^+$ diet for 16 h; and (C) Low Na$^+$ diet for 10 days.
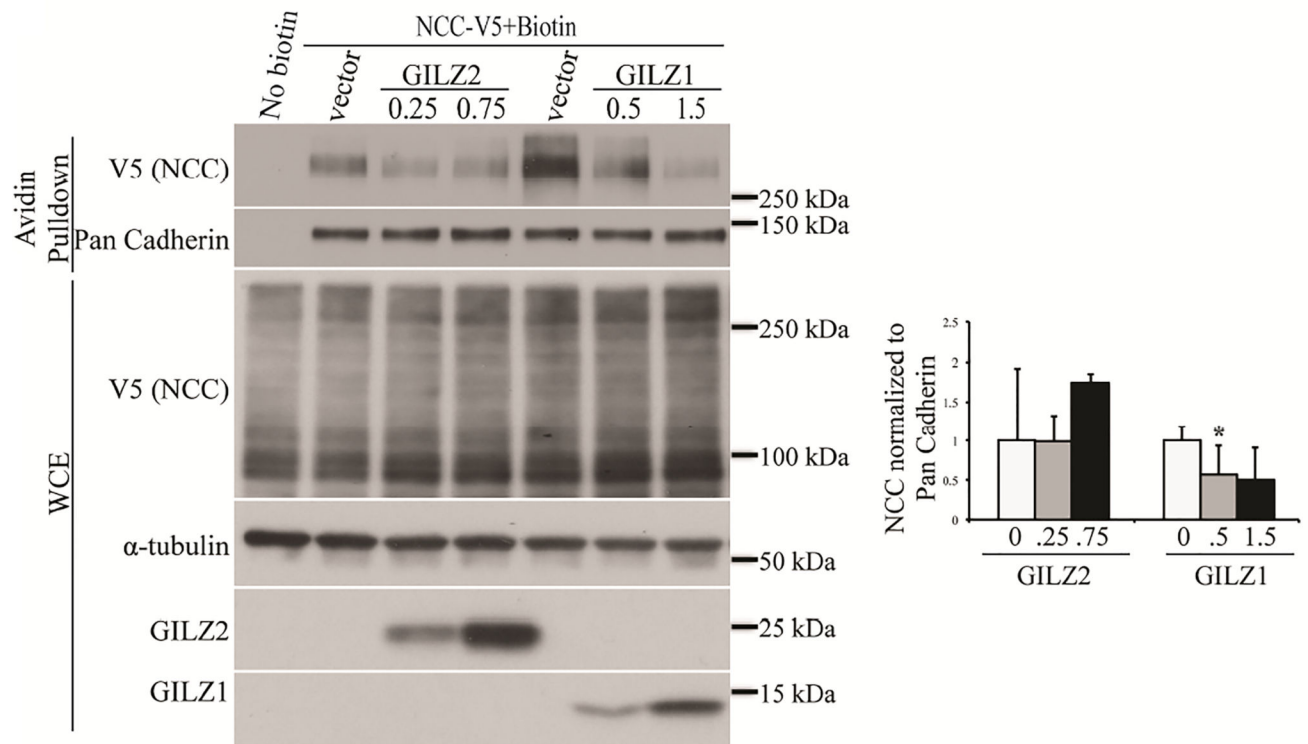
Figure 9. GILZ1 inhibits surface expression of NCC in HEK293T cells
HEK293T cells were transfected as indicated. Cell surface proteins were biotinylated and pulled down using avidin-conjugated beads. WCE: whole cell extract. Both dimeric and monomeric forms of NCC were detected in the whole cell extract while the dimeric form was predominant in the biotinylated fraction. Left: Representative blot. Right: Quantification of NCC surface expression from three independent experiments. Data represent mean ± SEM. p-value was calculated using bi-directional unpaired Student's t-test. *p-value<0.05.
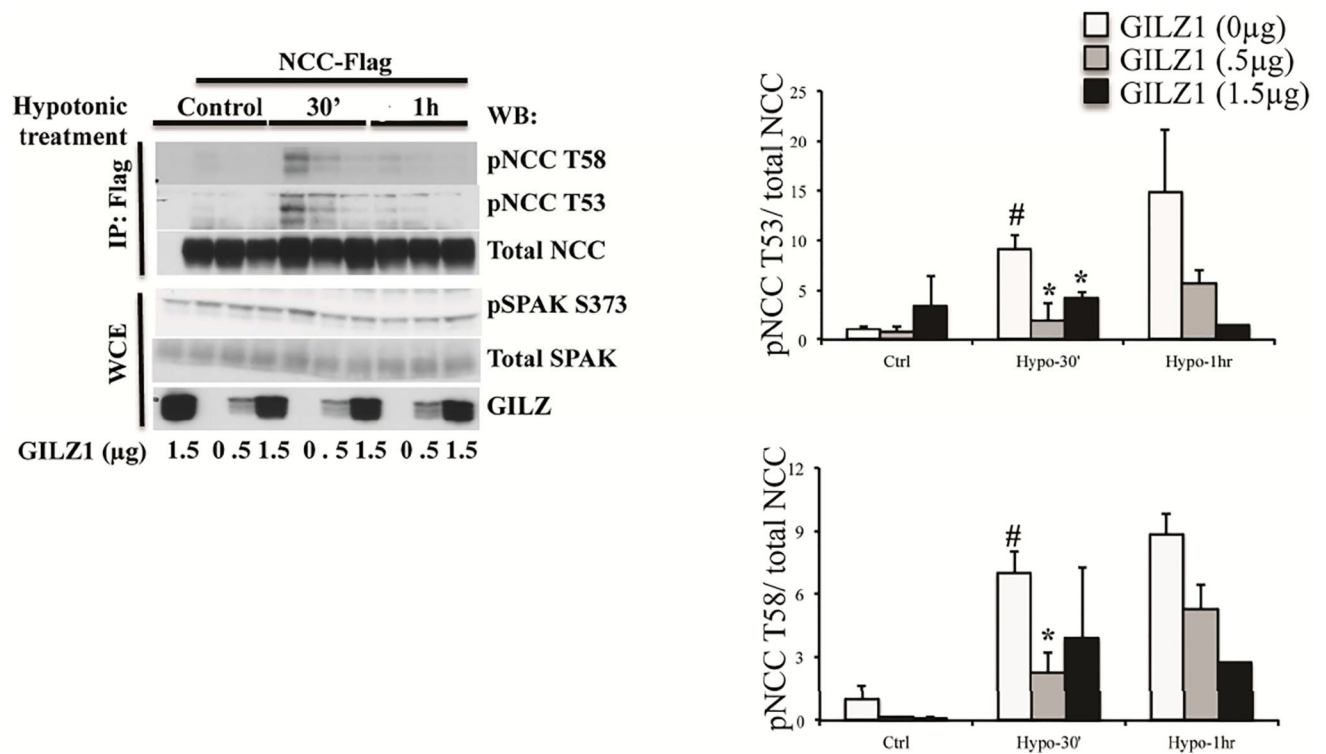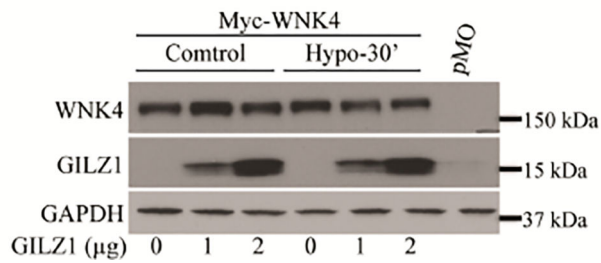
Figure 10. GILZ1 inhibits phosphorylation of NCC

HEK293T cells were transfected as indicated. 48 h after transfection, cells were treated with either basic control buffer or hypotonic low-Cl⁻ buffer for 30 min or 1 h. NCC was immunoprecipitated using Flag-conjugated beads and phosphorylation was assessed. WCE: whole cell extract. Left: Representative blot. Right: Quantification from three independent experiments. # p-value<0.05 with respect to control treated cells in the absence of GILZ, * p-value<0.05 with respect to pNCC T53/T58 levels after hypotonic treatment in the absence of GILZ.
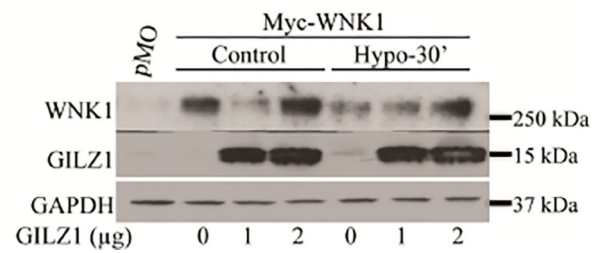
A.

B.

Figure 11. WNK4 and WNK1 levels remain unchanged in the presence of GILZ1
A. HEK293T cells were transfected with (A) Myc-WNK4; or (B) Myc-WNK1 in the presence of increasing amounts of GILZ1. 48 h after transfection, cells were treated with either basic control buffer or hypotonic low-Cl⁻ buffer for 30 min. Whole cell extract was prepared and WNK4 and WNK1 levels were assessed using anti-Myc antibody. Immunoblot shown is representative of three independent experiments with similar results.
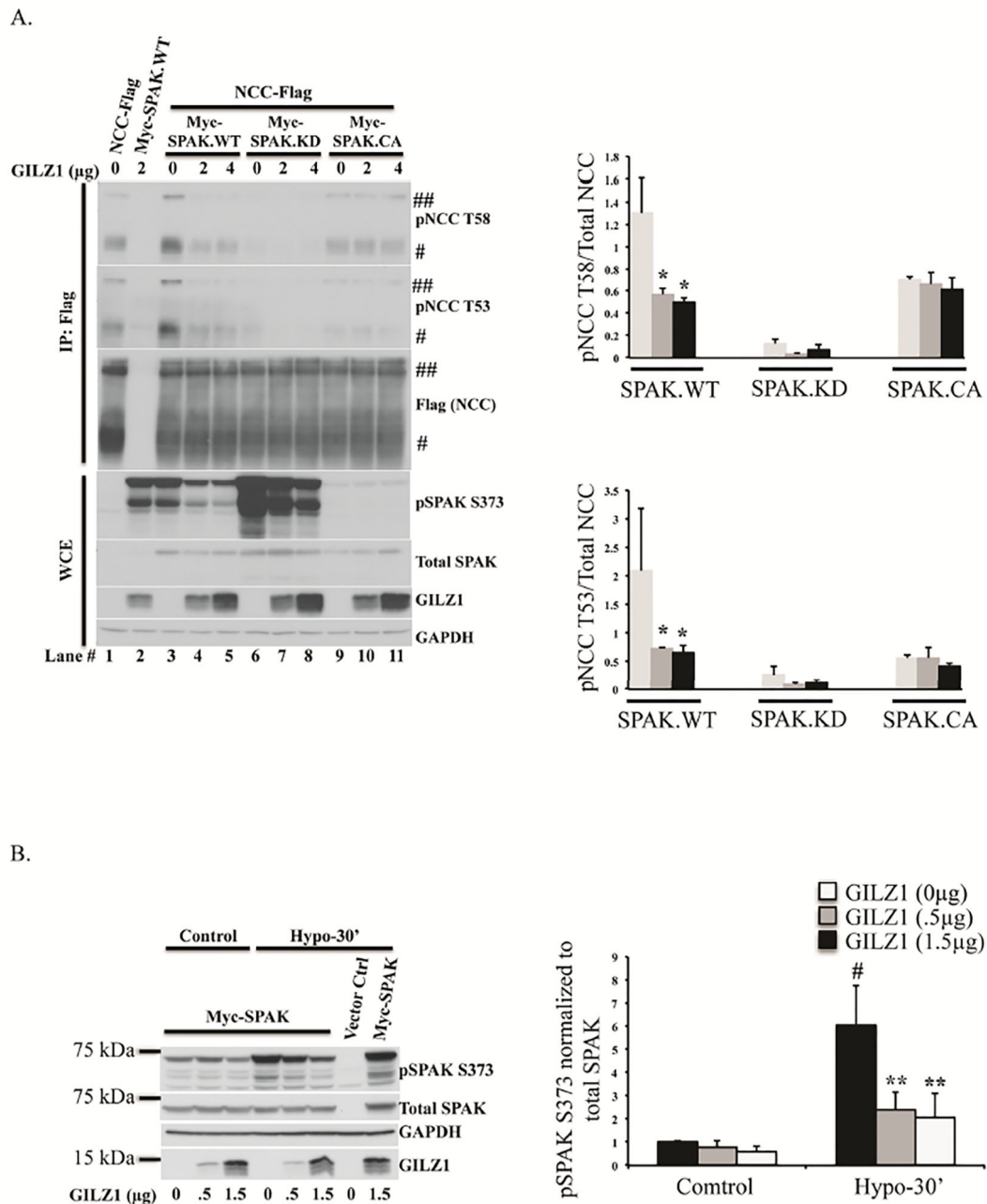
A.

B.

Figure 12. GILZ1 inhibits NCC through the SPAK pathway

A. HEK293T cells were transfected with Flag-tagged NCC in the presence of wild type (SPAK.WT), kinase dead (SPAK.KD) or constitutively active (SPAK.CA) SPAK as indicated. 48 h after transfection, cells were treated with either basic control buffer or hypotonic low-Cl⁻ buffer for 30 min. NCC was immunoprecipitated using Flag-conjugated beads and phosphorylation was assessed. WCE: whole cell extract. #NCC monomer, ##NCC dimer. Left: Representative blot. Right: Quantification of pNCC T58 (Top) and T53 (Bottom) from three independent experiments. Both monomeric and dimeric forms of NCC

were included in the quantification. Data represent mean ± SEM. p-value was calculated using bi-directional unpaired Student's t-test. *p-value<0.05.

B. HEK293T cells were transfected as indicated. 48 h after transfection, cells were treated as above and lysates were prepared. pSPAK S373 and total SPAK were assessed. Left: Representative blot. Right: Quantification of pSPAK S373 using four independent experiments. # p-value<0.05 with respect to pSPAK S373 levels in control buffer. # p-value<0.05 with respect to control treated cells in the absence of GILZ, ** p-value<0.005 with respect to pSPAK 373 levels after hypotonic treatment in the absence of GILZ.
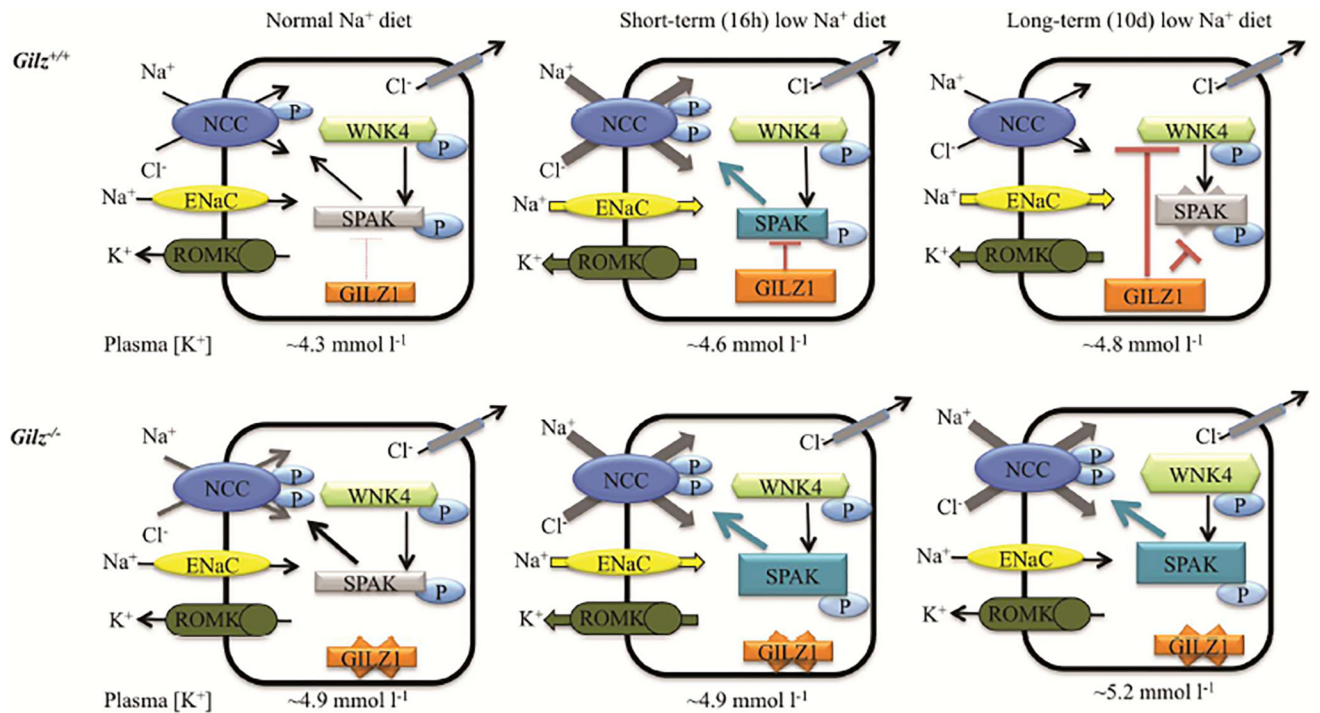
Figure 13. Model depicting GILZ mediated inhibition of NCC to modulate K$^+$ secretion
GILZ1 stimulates K$^+$ secretion through ROMK and BK$_{ca}$ (not shown in the model) channels by shifting Na$^+$ reabsorption away from NCC mediated electroneutral transport to ENaC mediated electrogenic transport. For simplicity, expression of NCC, ENaC as well as ROMK is shown in the same cell. Notably, cells with this pattern of expression may exist in DCT2. Upper panels: *Gilz*$^{+/+}$ mice; lower panels: *Gilz*$^{-/-}$ mice; left panels: normal salt diet; middle panels: 16h low salt diet (short term); and right panels: 10 days low salt diet (long term). Note also that the peak plasma [K$^+$] in the *Gilz*$^{+/+}$ animals is lower than the baseline plasma [K$^+$] in *Gilz*$^{-/-}$ (see text for details).

Table 1

Blood Pressure in $Gilz^{+/+}$ and $Gilz^{-/-}$ mice on normal Na$^+$ diet.

Parameter	$Gilz^{+/+}$ (n=7)	$Gilz^{-/-}$ (n=6)
Systolic (mm Hg)	149.3 ± 5.3	148.3 ± 2.4
Diastolic (mm Hg)	122.1 ± 4.4	120.3 ± 3.2
MAP (mm Hg)	130.8 ± 4.7	129.3 ± 2.9
Heart Rate (beats per minute)	468.1 ± 15.3	551.9 ± 12.8[*]

$Gilz^{+/+}$ and $Gilz^{-/-}$ mice (8–12 weeks old) were used to measure blood pressure by tail cuff method. MAP: mean arterial pressure; Values are mean ± SEM.

[*] $p < 0.05$ vs. $Gilz^{+/+}$.

Table 2

Physiologic blood parameters in *Gilz*^{+/+} *and Gilz*^{−/−} mice on normal Na^{+} diet.

Parameter	*Gilz*^{+/+} (n=8)	*Gilz*^{−/−} (n=10)
Body weight (g)	24.5 ± 0.58	24.4 ± 0.47
Food intake (g/g body wt. per 24 h)	0.13 ± 0.002	0.13 ± 0.005
Water intake (ml/g body wt. per 24 h)	0.15 ± 0.004	0.15 ± 0.007
Na^{+} (mmol/L)	146.6 ± 0.31	148.1 ± 0.57[*]
K^{+} (mmol/L)	4.3 ± 0.09	4.9 ± 0.10[**]
Cl^{−} (mmol/L)	110.1 ± 0.48	111.9 ± 0.41[*]
iCa[2+] (mmol/L)	1.2 ± 0.01	1.2 ± 0.01
TCO$_2$ (mmol/L)	22.6 ± 0.26	23.5 ± 0.34
Glucose (mg/dL)	233.9 ± 6.47	203 ± 8.6[*]
BUN (mg/dL)	21.6 ± 0.46	23 ± 0.88
Creatinine (mg/dL)	<0.2	<0.2
Hematocrit	39 ± 0.27	38.2 ± 0.42

Gilz^{+/+} and *Gilz*^{−/−} mice (8–12 weeks old) were acclimatized for three days in balance cages on normal Na^{+} diet. Blood was collected using retro-orbital bleeding. Blood electrolytes were measured using i-STAT. iCa[2+]: ionized calcium; TCO$_2$: total CO_2; BUN: blood urea nitrogen. Values are mean ± SEM.

[*] $p < 0.05$ vs. *Gilz*^{+/+};

[**] $p < 0.001$ vs. *Gilz*^{+/+}.

Table 3

Urinary parameters in $Gilz^{+/+}$ and $Gilz^{-/-}$ mice on normal Na^+ diet.

Parameter	$Gilz^{+/+}$ (n=8)	$Gilz^{-/-}$ (n=9)
Urine volume (μl/h)	69.7 ± 4.28	61.1 ± 4.55
Na^+ (mmol/L)	131.4 ± 7.43	133.4 ± 12.74
K^+ (mmol/L)	558.3 ± 25.29	565.4 ± 26.25
Cl^- (mmol/L)	406.6 ± 17.84	414.3 ± 22.89
Net Na^+ excretion (μmoles/h)	9.0 ± 0.42	7.8 ± 0.68
Net K^+ excretion (μmoles/h)	38.1 ± 1.56	33.3 ± 1.12
Net Cl^+ excretion (μmoles/h)	27.7 ± 1.00	24.2 ± 0.63 [*]
Na^+/K^+ ratio	0.24 ± 0.01	0.23 ± 0.02
Creatinine (mmol/L)	6.0 ± 0.39	6.6 ± 0.29
FE_{Na} (%)	0.15 ± 0.01	0.14 ± 0.01
FE_K (%)	22.21 ± 0.70	17.35 ± 0.47 [##]
Glucose (mg/dL)	148.63 ± 8.07	156.44 ± 7.28

$Gilz^{+/+}$ and $Gilz^{-/-}$ mice (8–12 weeks old) were acclimatized for three days in balance cages on normal Na^+ diet. Urine was collected for 16 h.

FE_{Na}: fractional excretion of Na^+, FE_K: fractional excretion of K^+. Values are mean ± SEM.

[*] p<0.05 vs. $Gilz^{+/+}$;

[##] p<0.00001 vs. $Gilz^{+/+}$.

Table 4

Urinary parameters in $Gilz^{+/+}$ and $Gilz^{-/-}$ mice on Na^+-deficient diet.

Parameter	16 h low-Na^+		24 h low-Na^+	
	$Gilz^{+/+}$ (n=13)	$Gilz^{-/-}$ (n=13)	$Gilz^{+/+}$ (n=8)	$Gilz^{-/-}$ (n=6)
Urine volume (μl/h)	47.2 ± 4.09	44.36 ± 2.49	24.8 ± 3.46	30.42 ± 3.95
Na^+ (mmol/L)	3.06 ± 0.34	2.23 ± 0.24	1.45 ± 0.48	0.75 ± 0.18
K^+ (mmol/L)	22.41 ± 1.85	26.5 ± 2.1	46.83 ± 6.36	44.12 ± 5.03
Cl^- (mmol/L)	8.66 ± 0.49	8.77 ± 0.43	9.86 ± 1.54	10.0 ± 0.70
Net Na^+ excretion (μmoles/h/g body wt.)	0.1 ± 0.01	0.07 ± 0.01[*]	0.013 ± 0.005	0.008 ± 0.003
Net K^+ excretion (μmoles/h/g body wt.)	0.72 ± 0.06	0.79 ± 0.06	0.41 ± 0.06	0.44 ± 0.04
Net Cl^+ excretion (μmoles/h/g body wt.)	0.27 ± 0.02	0.26 ± 0.01	0.04 ± 0.02	0.1 ± 0.009
Creatinine (mmol/L)	0.23 ± 0.02	0.25 ± 0.02	0.58 ± 0.07	0.53 ± 0.06
Glucose (mg/dL)	9.31 ± 0.57	10.25 ± 0.63	15.39 ± 2.03	12.92 ± 0.82

$Gilz^{+/+}$ and $Gilz^{-/-}$ mice (8–12 weeks old) were acclimatized for three days in balance cages on regular diet. Mice were then switched to a sodium deficient diet (0.01% NaCl) for 10 days. Urine was collected at indicated times. Values are mean ± SEM.

[*] $p < 0.05$ vs. $Gilz^{+/+}$.

Table 5

Physiologic blood parameters in $Gilz^{+/+}$ and $Gilz^{-/-}$ mice on Na$^+$-deficient diet.

Parameter	16 h low-Na$^+$		24 h low-Na$^+$	
	$Gilz^{+/+}$ (n=13)	$Gilz^{-/-}$ (n=13)	$Gilz^{+/+}$ (n=8)	$Gilz^{-/-}$ (n=8)
Na$^+$ (mmol/L)	146.3 ± 0.41	148.5 ± 0.82 *	146.1 ± 0.40	146.6 ± 0.32
K$^+$ (mmol/L)	4.6 ± 0.09	4.9 ± 0.15	4.85 ± 0.15	5.24 ± 0.07 *
Cl$^-$ (mmol/L)	110.0 ± 0.38	112.4 ± 0.75 *	113.9 ± 1.36	115 ± 1.31
iCa^{2+} (mmol/L)	1.2 ± 0.01	1.2 ± 0.01	1.1 ± 0.04	1.1 ± 0.05
TCO$_2$ (mmol/L)	24.1 ± 0.24	23.5 ± 0.33	22.3 ± 1.16	21.9 ± 0.83
Glucose (mg/dL)	207.7 ± 6.77	193.2 ± 5.53	197.9 ± 14.01	199.6 ± 27.69
BUN (mg/dL)	28.8 ± 0.93	30.7 ± 0.96	26 ± 3.16	27.6 ± 3.81
Creatinine (mg/dL)	0.22 ± 0.01	0.23 ± 0.02	0.3 ± 0.07	0.3 ± 0.07
Hematocrit	40.4 ± 0.47	39.3 ± 0.38	41.1 ± 0.83	40.4 ± 1.30

$Gilz^{+/+}$ and $Gilz^{-/-}$ knockout mice (8–12 weeks old) were acclimatized for three days in metabolic cages on standard diet. Mice were then switched to a sodium deficient diet (0.01% NaCl) for 10 days. Blood was collected using retro-orbital bleeding at indicated times. Blood electrolytes were measured using iSTAT. iCa^{2+}: ionized calcium; TCO$_2$: total CO$_2$; BUN: blood urea nitrogen. Values are mean ± SEM.

*
p<0.05 vs. $Gilz^{+/+}$.